Science of the Total Environment 907 (2024) 167951

Contents lists available at ScienceDirect

Science of the Total Environment

journal homepage: www.elsevier.com/locate/scitotenv

Effects of fir-wood biochar on CH_4 oxidation rates and methanotrophs in landfill cover soils packed at three different proctor compaction levels

Susan C. Yi [a,*], Anne Heijbroek [a], Luis Cutz [b], Stephanie Pillay [c], Wiebren de Jong [b], Thomas Abeel [c,d], Julia Gebert [a]

[a] Delft University of Technology, Faculty of Civil and Geosciences Engineering, Stevinweg 1, 2628 CN Delft, Netherlands
[b] Delft University of Technology, Faculty of Mechanical, Maritime and Materials Engineering, Leeghwaterstraat 39, 2628 CB Delft, Netherlands
[c] Delft University of Technology, Faculty of Electrical Engineering, Mathematics and Computer Science, Van Mourik Broekmanweg 6, 2628 XE Delft, Netherlands
[d] Broad Institute of MIT and Harvard, Infectious Disease and Microbiome Program, 415 Main St., Cambridge, MA 02142, USA

HIGHLIGHTS

- Compacted soil with biochar enhanced porosity and O_2 diffusivity, but not CH_4 oxidation.
- Compaction and biochar addition changed soil pore sizes.
- Biochar increased methanotrophs in sandy but not in clayey soil.
- The response of soil properties to biochar addition is equivocal and soil-specific.

GRAPHICAL ABSTRACT

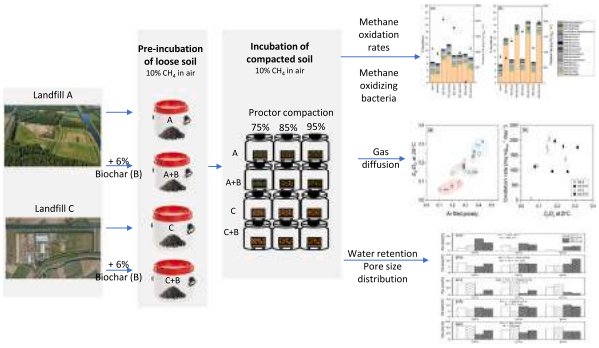

ARTICLE INFO

Editor: Frederic Coulon

Keywords:
Biochar
Proctor compaction
Gas transport
Landfill cover soil
Methane oxidation
Soil properties
Pore size distribution
Methanotrophs

ABSTRACT

Application of biochar to landfill cover soils can purportedly improve methane (CH_4) oxidation rates, but understanding the combined effects of soil texture, compaction, and biochar on the activity and composition of the methanotrophs is limited. The amendment of wood biochar on two differently textured landfill cover soils at three compaction levels of the Proctor density was explored by analyzing changes in soil physical properties relevant to methane oxidation, the effects on CH_4 oxidation rates, and the composition of the methanotrophic community. Loose soils with and without biochar were pre-incubated to equally elevate the CH_4 oxidation rates. Hereafter, soils were compacted and re-incubated. Methane oxidation rates, gas diffusivity, water retention characteristics, and pore size distribution were analyzed on the compacted soils. The relative abundance of methanotrophic bacteria (MOB) was determined at the end of both the pre-incubation and incubation tests of the packed samples. Biochar significantly increased porosity at all compaction levels, enhancing diffusion coefficients. Also, a re-distribution in pore sizes was observed. Increased gas diffusivity from low compaction and amendment of biochar, though, did not reflect higher methane oxidation rates due to high diffusive oxygen fluxes over the limited height of the compacted soil specimens. All soils, with and without biochar, were strongly dominated by Type II methanotrophs. In the sandy soil, biochar amendment strongly increased MOB abundance,

* Corresponding author.
E-mail address: S.C.Buisma-Yi@tudelft.nl (S.C. Yi).

https://doi.org/10.1016/j.scitotenv.2023.167951
Received 12 June 2023; Received in revised form 17 October 2023; Accepted 18 October 2023
Available online 19 October 2023

which could be attributed to a corresponding increase in the relative abundance of *Methylocystis* species, while no such response was observed in the clayey soil. Compaction did not change the community composition in either soil. Fir-wood biochar addition to landfill cover soils may not always enhance methanotrophic activity and hence reduce fugitive methane emissions, with the effect being soil-specific. However, especially in finer and more compacted soils, biochar amendment can maintain soil diffusivity above a critical level, preventing the collapse of methanotrophy.

1. Introduction

Landfills contribute significantly to global anthropogenic methane (CH_4) emissions (IPCC, 2021), with ~16 % of total CH_4 emissions in the Netherlands originating from anaerobic degradation of organic matter in landfills (RIVM, 2021). The global warming potential (GWP) of CH_4 is 28 over 100 years and as high as 84 over 20 years (IPCC, 2021), making landfills a priority sector that necessitates a reduction of climate forcing emissions. One option is to optimize microbial oxidation of CH_4 in landfill biocovers, complimenting active gas extraction systems to fully reduce the long-term low-calorific methane fluxes after active gas extraction terminates (Gebert et al., 2022; Huber-Humer et al., 2008; Scheutz et al., 2009). Landfill biocover technology promotes the activity of methane-oxidizing bacteria (MOB) by enhancing soil properties favorable to methanotrophic activity. These include soil physical properties that govern water retention (Boeckx et al., 1996; Czepiel et al., 1995; Scheutz and Kjeldsen, 2004), surface area for bacterial colonization and gas transport (Hill et al., 2019; Keiblinger et al., 2015; Rockhold et al., 2004), and geochemical properties that regulate soil pH and nutrient supply (De Visscher et al., 1999; Hilger et al., 2000).

Previous research has shown the effects of pH (Hanson and Hanson, 1996; Scheutz and Kjeldsen, 2004), nutrient limitations (De Visscher et al., 1999; Scheutz et al., 2009) and extracellular polymeric substances (Wilshusen et al., 2004) on CH_4 oxidation. Furthermore, temperature, moisture content, porosity, and previous methane exposures are environmental conditions that also affect landfill methane oxidation rates (Börjesson et al., 2004; Gebert et al., 2003; Park et al., 2005). Materials such as compost, sand, green wastes, or wood chips are also often added to landfill biocovers to maintain high air-filled porosities for optimized diffusion of atmospheric oxygen into the soil necessary to convert CH_4 into H_2O and CO_2, and to retain moisture contents favorable to microbial activity.

Biochar is an alternative organic-rich material for biocover amendment suggested to increase the population of methanotrophic bacteria and methane oxidation rates in landfill cover soils (Reddy et al., 2014, 2021; Yargicoglu and Reddy, 2017a, 2018; Yargicoglu and Reddy, 2017b). It is a byproduct of pyrolysis of organic materials or biowastes that have undergone thermochemical conversion in oxygen-limited conditions (Lehmann and Joseph, 2009) that can be added to soils with the potential for improving soil properties, enhance pollutant retention and or transformation, or water retention and infiltration. Compared to compost, biochar is characterized as more recalcitrant and hence offers structural stability over a longer time. Therefore, biochar can be utilized as an alternative substrate for promoting the growth of methanotrophs, which in turn helps to reduce CH_4 emissions in landfill cover soils.

Several factors that drive methane oxidation complicate the understanding of the effects of biochar on landfill cover soils. One of the major factors regulating methane oxidation is the availability of oxygen, governed by soil gas transport properties (Gebert et al., 2011; Mostafid et al., 2012), which are in turn moderated by soil moisture which can either be reduced by decreasing gas transport rates (Poulsen et al., 2008; Schjonning et al., 2003) or enhanced by increasing microbial activity. Recent studies and models have shown that biochar can increase or decrease water retention at different matric potentials and for different biochar and soil texture combinations. Soil gas transport is reduced by soil compaction (Poulsen et al., 2008; Verseveld and Gebert, 2020), leading to a decline in methane oxidation rates, as, for example, shown in a landfill cover-simulating column study (Gebert et al., 2011; Rachor et al., 2013).

The current US landfill operating practices require compacting and covering waste with soil to reduce odors and fires, control disease vectors, minimize litter scattering, and protect human health and the environment (US EPA, 1997). There is no established regulation regarding specified Proctor compaction levels in the US, Germany, and the Netherlands, thus allowing flexibility in certain site-specific situations and soil types. The US regulation specifies performance standards for the landfill cover soil by directing the operators to keep the cover soil dry by reducing infiltration and erosion by compacting the soil to minimize the "bathtub effect," which is to minimize water entering into the waste bodies that can have leachate overproduction, potentially causing groundwater contamination (US EPA, 1997). According to the German Landfill Ordinance, compaction is minimized to achieve an air capacity of a minimum of $8\%_{vol}$ at an available water capacity of 220 mm to enhance vegetation growth and not exceed water seepage of 60 mm per year (Anlauf and Rehrmann, 2012).

Soil compaction modifies pore size distribution, pore arrangement, and soil pore interconnection (Lipiec et al., 2012), resulting in reduced water holding capacity (Hajnos et al., 2006), thereby altering gas transport properties, reducing hydraulic conductivity (Berisso et al., 2012; Watabe et al., 2000), and decreasing the methanotrophic activity (Sleutel et al., 2012; Verseveld and Gebert, 2020). Soil compaction can restrict access to oxygen and water to the microbial community, potentially causing adverse effects and reducing methane oxidation rates. The magnitude of the effect and thereby the impact on the soil's capacity to oxidize CH_4 is dependent on the soil texture. When biochar-amended soils are compacted, the static energy released on the soil can break the biochar particles, reducing void spaces, therefore changing pore size classes exerting capillary effects, modifying water retention, and gas transport rates.

It is crucial to understand the influence of biochar particles on differently textured soils under various compaction levels to assess the potential of biochar amendment to landfill cover soils for enhancing the reduction of methane emissions from landfills. Currently, there is a paucity of information about the effects of biochar on standard Proctor test to understand compaction conditions on optimum water content and the underlying impact on methane oxidation. This study aims to elucidate the effect of fir tree biochar addition on methane oxidation in a sandy and clayey landfill cover soil collected from two landfills in the Netherlands under different Proctor compaction levels following previous works (Anlauf and Rehrmann, 2012; Van Verseveld, 2018). It was hypothesized that biochar enhances methane oxidation in these soils by increasing porosity, thus, increasing gas diffusivity, and that the effect is more pronounced with higher levels of compaction. To isolate the impacts of porosity on methanotrophy, soil moisture contents were maintained at a constant level since a beneficial effect of enhanced water retention was expected, particularly in sandy soils.

2. Material and methods

2.1. Landfill cover soils and biochar

Landfill cover soils were collected from Wieringermeer landfill (Middenmeer, The Netherlands) and Braambergen landfill (Almere, The

Netherlands) operated by Afvalzorg Deponie B.V. Both soils had been previously exposed to methane, where Braambergen soil (Soil A) was an active landfill cover soil in direct contact with the waste body without an intercepting surface liner, while Wieringermeer soil (Soil C) had been used as a biocover test field. The particle size distribution curves were obtained on both landfill soils to determine the USDA soil textures (ASTM, 2006).

Biochars were purchased from Pyropower (Delft, Netherlands), where they were produced from recycled Christmas (fir) trees using a slow pyrolysis system at 500 °C. Biochars were sieved to 2 mm particle size prior to soil amendment to ensure particle size uniformity and minimize soil texture changes. Ultimate analyses determining the main elemental compositions (C, H, N, S, O) were performed on the sieved biochar in duplicate using a EuroVector EA3400 Series CHN-O analyzer with acetanilide as the reference (Supplementary Information). The oxygen contents were determined by the difference. Inductively coupled plasma optical emission spectrometry (ICP-OES) was also performed on the biochar by digesting them in aqua regia and H_2O_2 on a heat plate. Data on elemental contents were acquired using a Spectro-Arcos EOP combined with Spectro Smart Analyzer Vision software (Table S2 in Supplementary Information). Scanning electron microscopy images (Fig. S2 in Supplementary Information) were also recorded using a backscattered electron detector in a compositional mode with an accelerated voltage of 10 kV and beam current of 65 pA (Del Grosso et al., 2022).

Proximate analysis was performed, and the results are presented in Table S4 in Supplementary Information. The moisture content was obtained using a moisture analyzer and the volatile matter (VM) was determined using a thermogravimetric analyzer (TGA – SDT Q600) (Del Grosso et al., 2022). The ash content was acquired in accordance with NREL/TP-510-4262. The fixed carbon was then calculated by the difference.

N_2-physisorption tests were conducted on a Quantachrome Instruments' NOVAtouch™-LX gas sorption analyzer with high purity N_2 (99.99 %) at 77 K to obtain the Specific Surface Area (SSA). Before measuring, the samples were degassed at 130 °C for 16 h. Each test was performed in duplicate. SSA was calculated by applying the Brunauer-Emmett- Teller (BET) method. Adsorption branches between 0.05 and 0.20 relative pressure (P/P_0) were used to determine the SSA. The pore volume of the biochar was estimated using the Density-Functional Theory (DFT) method. The results are found in Supplementary Information, section S2.3.

Soils and biochar were air-dried in an ambient condition prior to any mixing, and an aliquot of the materials was oven-dried at 105 °C overnight to determine the moisture content. The air-dried gravimetric water contents were 0.6 % for Soil A and 1.3 % for Soil C. The samples were not oven-dried to maintain the methane-oxidizing bacteria, and the air-dried soil lumps were broken down using a mortar and pestle before the start of experiments.

All air-dried cover soils were manually mixed with 2 mm sieved biochar at 6 % (d*w*/w) to provide a homogenous mixture. Biochar contents of 6 % were chosen because biochar application to soil can produce neutral or undesired hydrological outcomes as it can predominantly change soil structure and soil-water properties. For example, it was shown that biochars have transient wettability, sometimes leaching hydrophobic compounds and/or changing the soil-water interface at high (>15 % w/w) biochar application rates (Yi et al., 2015). A recent review paper reported that biochar has the potential to reduce soil fertility and release toxic substances that can adversely affect soil organisms (Brtnicky et al., 2021), similar to the effects of excessive fertilizer application on the reduction of soil quality. Therefore, 6 % biochar was used, which is an agriculturally relevant application amount (Mckay et al., 2021), and to ensure no physico-mechanical properties were changed (Das et al., 2015).

The 5 g of each sample were pelletized using a manual sample press and analyzed for total carbon (TC) (Unicube Elemental Analyzer, Langenselbold, Germany). The pH and electrical conductivity (EC) were also measured (Consort C1010 multi-parameter analyzer, Turnhout, Belgium) on solutions prepared using 10 g of sample mass with 40 g of deionized water that was allowed to stand for 24 h before collecting the measurements. Total inorganic carbon was estimated by taking 1 g of sample and saturating it with 40 % H_3PO_4 for 24 h at 80 °C in 250 cm^3 in a glass bottle. The $CO_2\%_{vol}$ contents and pressure were measured and calculated for total inorganic carbon. Total organic carbon was estimated by subtracting the total inorganic carbon after determining the C loss from the acidification of the samples. All samples were prepared and measured in duplicate.

2.2. Compaction tests

The standard Proctor test (ASTM, 2021) was performed on air-dried Soil A, Soil A + B, Soil C, and Soil C + B to obtain the optimum water content (W_{opt}) and the Proctor density (D_{Pr}) to obtain the compaction curves (Supplementary Information, Fig. S1). The Proctor density reflects the highest degree of compaction, i.e., the highest bulk density (ρ_b), that can be achieved using the Proctor energy at the optimum moisture content (the moisture content at which soil attains the maximum dry density).

Compaction behavior depends on particle size distribution, water content, anisotropy, and layer thickness (Anlauf and Rehrmann, 2012; Pulat and Yukselen-Aksoy, 2013; Romero and Jommi, 2008). In order to compare methane oxidation rates and soil properties for both soils in relation to their specific compaction behavior, and to cover a range of bulk densities found in the field, soils were compacted to the same level of their respective Proctor density, in this case 75 %, 85 %, and 95 % of the Proctor density.

For each step of water addition, new material was used to avoid irreproducible compaction curves (Lamprinakos and Manahiloh, 2019). For the measurement of the methane oxidation rate after the pre-incubation, and for the determination of the water retention curve, all soils were compacted to bulk densities corresponding to the relative compaction levels (C_R) of 75 %, 85 %, and 95 % of the Proctor density (Eq. (1)).

$$C_R = \frac{\rho_b}{D_{Pr}}\ x\ 100\% \tag{1}$$

2.3. Establishing soil moisture contents of loose and compacted soil samples

The respective water retention curves corresponding to their compaction at 75 %, 85 %, and 95 % D_{Pr} were estimated using the van Genuchten model (Moldrup et al., 2005a; van Genuchten, 1980) to determine the water contents of the two loose soils A and C. The average hydraulic parameter values, the residual water content (θ_r), and the saturated water content (θ_s) were estimated from Eqs. (2) and (3) using the quantity of clay, TOC, and the dry bulk density (ρ_b) from Eq. (1) of the two control soils at 75 %, 85 %, and 95 % D_{Pr} (Moldrup et al., 2005b; van Genuchten, 1980; Vereecken et al., 1989).

$$\theta_r = 0.015 + 0.005\ clay + 0.014\ TOC \tag{2}$$

$$\theta_s = 0.81 - 0.283\ \rho_b + 0.001\ clay \tag{3}$$

The water content corresponding to a capillary pressure of 1000 hPa at the reference (medium) compaction of 85 % D_{Pr} was chosen to be the gravimetric moisture contents for the three compaction rates since the moisture contents varied the least and were statistically insignificant between the three Proctor compaction levels after comparing the water contents between 300 hPa and 1000 hPa. Furthermore, the intention was also to keep the moisture level drier than the field capacity to eliminate any possibility of free water drainage. Taking the uncertainties between the two soil types into account, 1000 hPa was chosen to provide

a condition that is not excessively dry and not too wet, allowing for a comfortable margin away from the available water content of 300 hPa.

A gravimetric water content of 17.8 % (w/dw) was estimated to correspond to capillary pressure of 1000 hPa at 85 % D_{Pr} for the Soil A/A + B, and it was 5.9 % (w/dw) for the Soil C/C + B. These calculations were related to soils without biochar. It is well established that biochar can change water holding capacity in soils (Marsiello et al., 2015). Therefore, maintaining the same water moisture level throughout the experiment enabled isolating the effect of water retention changes due to biochar amendment on methane oxidation.

To meet the same moisture content throughout the study, the sample holding containers were weighed daily, and the weight change was an indicator of water increase or decrease. When there was a water loss during the pre-incubation stages, water was added and mixed with the loose soil to meet the reference weight. In the compacted samples, the moisture contents were kept constant by pipetting deionized water droplets onto the top of the compacted samples when the weight decreased. When there was a weight increase (both during pre-incubation/incubation stages), water was evaporated by opening the lid of the container and monitoring the weight change over time. The water evaporation time was less than <8 h since the water produced from methane oxidation was less than ~1 % of the initial weight. Because the containers were tightly sealed, modifying the water contents by evaporation were seldom performed.

The gravimetric water contents for Soil A/A + B were maintained at 17.8 % during the entire study for the loose soils and after compacting to 75 %, 85 %, and 95 % D_{Pr}. The gravimetric water contents for Soil C/C + B were initially established at 5.9 % (w/dw) during the pre-incubation stages of the loose soils but then increased and maintained to 7.7 % (w/dw) after 70 d of the pre-incubation step when there was no response in the methane oxidation rates (Fig. 3). The gravimetric moisture contents of Soil C and Soil C + B were 7.7 % (w/dw) for all three compaction levels. The samples were then tested to monitor the effect of compaction on biochar-amended landfill cover soils on methane oxidation capacity (Section 2.4), soil diffusivity (Section 2.6), and pore size distribution via water retention (Section 2.7). The effects of biochar amendment and compaction on the methanotrophic community were additionally assessed by DNA analyses of the loose and compacted soils at the end of the incubation period (Section 2.5). The details are found in the following sections.

2.4. Methane oxidation capacity

Once the control soils and biochar-amended landfill cover soils were adjusted to a target water content corresponding to a matric potential of ~1000 hPa at 85 % Proctor density (Section 2.3), ~5 kg dry mass of each soil (A, A + B, C, C + B) were then pre-incubated to build up the methane oxidation capacity in a loose state in an airtight 26 l container by injecting an equivalent to 2.6 l of pure CH_4 (99.9 % purity) into the airtight 26 l container to achieve a concentration of ~10%$_{vol}$ at 19–20 °C. The CH_4 consumption was monitored by gas chromatographic analyses of the headspace (Agilent Technologies 490 Micro-GC, Santa Clara, CA, USA). When methane was depleted (~1%$_{vol}$ CH_4), the starting concentration was re-established by flushing the container with ambient air, mixing the soil, and reinjecting a 2.6 l pure methane to establish ~10%$_{vol}$ CH_4. If the moisture contents changed, water droplets were added or evaporated in ambient conditions to meet the established moisture content as described in Section 2.3. Each repeated injection of CH_4 is referred to as a phase. The methane oxidation capacity development was continuously monitored, and the pre-incubation study lasted 105 d, consisting of 23 phases for Soil A and Soil A + B and 19 phases for Soil C and Soil C + B. The purpose of pre-incubating the samples was to isolate the effect of compaction and biochar amendment on methane oxidation by providing all soils with the same starting condition, i.e., a maximum methane oxidation capacity (Amaral et al., 1998; Kightley et al., 1995; Spokas and Bogner, 2011).

Each pre-incubated soil was then compacted into metal cylinders (with a volume of ~103 cm^3 ± 2.8 standard error (S.E.)) in triplicate at 75 %, 85 %, 95 % of the Proctor density at a gravimetric moisture content of 17.8 % for Soil A and Soil A + B, and 7.7 % moisture content for Soil C and Soil C + B. The bulk densities, solid volumes, water contents, gas volumes, and total porosities are presented in Table 2. These samples were then placed in an airtight ~1 l containers and injected with ~10%$_{vol}$ CH_4 (100 ml 99.9 % CH_4) and reinjected when the CH_4 gas in the headspace fell below 1%$_{vol}$, following the procedure described above for the pre-incubation period. Again, the weights of the samples were monitored to maintain the moisture content throughout the incubation period. After 58 to 73 d, the CH_4 oxidation rate reached an asymptotic plateau, and the incubation stage terminated. The CH_4 oxidation rate per g of dry mass ($CH_{4,oxidation\ rate}$) was calculated using Eq. (4), and the average of the oxidation rates are reported using the % (v/v) concentration of CH_4:

$$CH_{4,oxidation\ rate} = \frac{\left|\frac{\Delta C}{\Delta t}\right| V M_{CH_4}}{V_m M} \quad (4)$$

where $|\Delta C/\Delta t|$ is the absolute value of the slope between the changes in methane concentration ΔC (%v/v) over the change in time (Δt), respectively. Oxidation rates were only calculated over the linear part of the slope with a Pearson's coefficient > 0.97, hence representing zero-order oxidation rates. V is the gas volume [l], M_{CH4} is the molar mass of methane (16 g mol^{-1}), V_m is the molar volume [l mol^{-1}] assumed to be 24.0 l mol^{-1} at 293 K, and M is the dry mass [g] of the sample.

The actual oxygen fluxes ($J_{O_2 exp}$) in the compacted samples were also calculated using the measured CH_4 oxidation rates:

$$J_{O_2,exp} = CH_{4,t=final}\ \rho_b\ x\ \frac{M_{O_2}}{M_{CH_4}} \quad (5)$$

where $CH_{4,t=final}$ is the averaged oxidation rate of the compacted soil from the last three phases of the incubation experiments (at 58–73 d), ρ_b is the dry bulk density of each compacted sample, x is the half depth of the sample column (2.5 cm), and the last two factors (including the stoichiometric factor for O_2) are the molar mass of oxygen, M_{O_2}, and M_{CH_4} is the molar mass of CH_4.

2.5. Identification of methane oxidizing microorganisms (NGS and 16S-qPCR)

At the end of the pre-incubation period (loose soil) and the end of the incubation experiment (compacted samples), soils were homogenized, and ~ 10 g of each sample was sent to BaseClear B.V. (Leiden, the Netherlands), where 0.15 g were used for DNA extraction for methanotrophic community composition using Next Generation Sequencing (NGS) and 16S qPCR analyses.

The metagenomic DNA read data were generated using Illumina NovaSeq 6000 paired-end sequencing. Initial quality assessment was done using Illumina Chastity filtering. Further quality control was done using FastQC (Andrews, 2013). Reads were filtered using Trimmomatic v.0.39 (Bolger et al., 2014) and adaptors were removed while specifying *LEADING:3 TRAILING:3 MINLEN:35 SLIDINGWINDOW: 4:20 CROP: 140* parameters. Quality was then reassessed using FastQC. The methanotrophic community was profiled using the K-mer based Kraken2 v2.1.0 (Wood et al., 2019) using the minikraken2 microbial database (2019, 8GB). Thereafter, species confirmation and the estimation of abundance was done by Bracken v2.6.2 (Lu et al., 2017). Relative abundances of the methanotrophic community were normalized using the quantity target per µl DNA and used for downstream analyses.

The qPCR analyses were performed on 384 well PCR plates (Thermo Fisher Scientific, Waltham, MA, USA) sealed with MicroAmp Optical Adhesive Film (Thermo Fisher Scientific, Waltham, MA USA) using an Applied Biosystems QuantStudio™ 5 Real-Time PCR system (Thermo

Fisher Scientific, Waltham, MA, USA) with QuantStudio™ Design & Analysis software v1.4.2.

Each reaction for the total bacteria qPCR assay targeting the 16S rRNA gene was carried out in a total volume of 10 μl, with 5 μl ABsolute™ Blue qPCR Mix, Low ROX (Thermo Scientific, Waltham, MA, USA), 0.2 μl forward primer (5′-CGGTGAATACGTTCYCGG-3′; 10 μM), 0.2 μl reverse primer (5′-GGWTACCTTGTTACGACTT-3′; 10 μM), 0.1 μl probe (FAM-CTTGTACACACCGCCCGTC-BHQ1; 10 μM), 2 μl PCR grade water, and 2.5 μl undiluted template DNA. A standard curve comprising 8 serial 10-fold dilutions of a synthesized, cloned, linearized, and purified DNA of 192 bp was generated from a work solution (0.1 ng μl^{-1}) that in turn was derived by 100 times diluting a stock solution (10 ng μl^{-1}). The PCR program started with a denaturation step at 95 °C for 15 min, followed by 40 cycles consisting of denaturation at 95 °C for 15 s, annealing and elongation at 52 °C for 1 min with data collection.

A positive control was performed alongside each separate amplification consisting of 2.5 μl of 0.1 ng μl^{-1} DNA (0.25 ng DNA added to a single reaction) that was derived from ZymoBIOMICS™ Microbial Community DNA Std. (D6306; Zymo Research, Irvine, CA, USA). Negative template control (NTC) PCRs were performed alongside each separate amplification without addition of template. Amplification data were exported from QuantStudioTM Design & Analysis software v1.4.2 followed by determining the target quantity per μl DNA preparations using the standard curves and calculation of the number of targets per gram or ml of raw material. The resulting quantity target copies per μl DNA were corrected for the dilution factor and the quantity target copies per gram of material were calculated.

2.6. Gas diffusivity

Diffusion tests were performed on the compacted samples in 250 cm^3 steel cores (Table 3) in duplicate using a gas chamber equipped with an INIR-ME-100 % infrared methane sensor (SGX Sensortech, Neuchatel, Switzerland). After a leakage test of the apparatus was performed, a sample core was placed on top of a gas chamber fitted with a sliding plate. The gas chamber was first flushed with synthetic landfill gas (CH_4/CO_2) mixture for 30 s to set the initial concentration (C_0) inside the chamber. Then 1.5 ml of C_2H_2 was injected into the chambers to cease the activity of methanotrophic bacteria consuming CH_4. Once a constant CH_4 concentration was established, the sliding plate was opened to allow gas to diffuse through the sample core. Fick's first law was used to calculate the effective gas diffusion coefficient to monitor the change in CH_4 concentration inside the chamber over time of methane (Dane and Topp, 2002) in Eq. (6),

$$C_{CH_4} = (C_0 - C_{atm}) exp^{-D_p \frac{At}{Vl}} + C_{atm} \quad (6)$$

where C_{CH_4} is the concentration of CH_4 measured by the sensor, C_0 is the initial concentration of CH_4 in the gas chamber, C_{atm} is the methane concentration in the atmosphere (1.76 mg l^{-1}), D_p is the effective gas diffusion coefficient, A is the area of the sample core where diffusion is occurring, t is the time, l is the length of the soil sample, and V is the volume of the chamber. The effective gas diffusion coefficient was then normalized with the diffusion coefficient of methane in air at a laboratory temperature of 20 °C (0.21 $cm^2\ s^{-1}$) to obtain the gas diffusivity (D_p/D_o). More details can be found in Gebert et al. (2019). Dividing the D_p by the air-filled porosity (ε) yields the specific diffusivity ($D_s = D_p/\varepsilon$), and estimating the potential diffusive transport of oxygen through the soil samples,

$$J_{O_2 potential\ flux} = D_p \frac{dC}{dx} M_{O_2} \quad (7)$$

was used (Table 3, $J_{O2\ potential\ flux}$), assuming gas transport to the middle of the sample ring ($dx = 2.5$ cm) using a concentration of $dC = 9.37$ mol $O_2\ m^{-3}$ (equals 21 % O_2 in air), then multiplied by the molar mass of O_2 (M_{O_2}) to obtain the units of g $O_2\ m^{-2}\ d^{-1}$. Based on the J_{O2} potential flux, the maximum CH_4 flux that can be oxidized was calculated (J_{CH4} potential flux in Table 3), assuming that the oxidation of one mol of CH_4 requires two mols of O_2 and compared to the actually measured CH_4 oxidation rate (J_{CH4} oxidized). Similarly, Eqs. (7) and (5) were used to obtain the sample depth (dx) at which the O_2 supply would get depleted, $dx = D_p \frac{dC}{J_{O_{2,exp}}}$, where $J_{O2,\exp}$ is the actual O_2 flux obtained from the CH_4 oxidation rate at the end of the incubation stage of the compacted samples (eq. 5).

2.7. Water retention curve and pore size distribution

The duplicate compacted samples in ~250 cm^3 used for the diffusion tests were slowly saturated with de-aired, deionized water in 1 cm increments hourly until the water level reached a level close to the rim of the sample packing. They were then saturated overnight in the de-aired and deionized water bath with a loosely fitted lid to minimize evaporation for obtaining the soil water retention curves (SWRC). The water retention curves were collected for each sample at the three compaction levels using the Hyprop apparatus (Meter Group, Inc., Pullman, WA, USA) at 0 to 1000 hPa suction pressure range to analyze the effects of compaction on pore size distribution and CH_4 oxidation rates. The measurements at the dry ends of the water retention curves were collected using a WP4C dewpoint potentiometer (Meter Group Inc. Pullman, WA, USA).

Using the SWRC, the Young-Laplace equation was adopted to calculate the pore radius at each capillary pressure step assuming cylindrical pores corresponding to the pore opening:

$$r = \frac{2\sigma\ cos\alpha}{\Delta P} \quad (8)$$

where d is the diameter [m], ΔP is the capillary pressure [N m^{-2}], σ is the surface tension of water (0.072 N m^{-1}) is water, α is the contact angle between particle and water assuming 0°. The direct pore size distribution was then obtained using the derivative $f(r)$ in Eq. (8) using the volumetric water content (θ) (Nimmo, 2004):

$$f(r) = \frac{d\theta}{dr} \quad (9)$$

2.8. Statistical analysis

Single-factor ANOVA tests were performed on samples incubated in loose conditions and samples corresponding to the compaction level to determine the differences between the means of soil to the soil+biochar mixtures on CH_4 oxidation. The results were then compared using the two-sample t-test assuming equal variances to obtain p-values (error probability) of 0.05 to determine whether differences were statistically significant. If $p < 0.05$, the differences of the mean were considered significant. The statistical analyses were conducted using Microsoft Excel (Microsoft, Redmond, WA, USA).

3. Results

3.1. Soil properties

3.1.1. Loose soils: soil texture, proctor density, and optimum water content

3.1.1.1. Landfill cover soil. Soil A is a finer soil containing significantly more clay and silt; and, consequently, less sand than Soil C, with a coarse texture (Table 1). Soil compaction tests showed a slightly higher Proctor density in Soil C than in Soil A but a lower optimum water content. The total carbon contents were slightly higher in Soil A than in Soil C, and the TC/TN ratio was lower in Soil A than Soil C. Electrical conductivity, representing soil salinity, was slightly higher in the fine-grained Soil A, and the pH values did not deviate between the samples.

Table 1
Properties of biochar and landfill cover soils from Wieringermeer[a] (Verseveld and Gebert, 2020), Braambergen (Holland and Gebert, 2020) and their respective biochar mixtures.

Soil Property	Units	Biochar	Braambergen (Soil A)	Braambergen + Biochar (Soil A + B)	Wieringermeer (Soil C)	Wieringermeer + Biochar (Soil C + B)
Clay (d < 0.002 mm)	% dw	–	21	20	8.8	8.3
Silt (0.002 mm < d < 0.05 mm)	% dw	0.04	52	49	7.2	10.7
Sand (0.05 mm < d < 2.00 mm)	% dw	2.5	27	31	82.4	81
Gravel (d > 2.00 mm)	% dw	97	0	0	1.6	0
USDA texture class	–	–	SiL	SiL	LS	LS
Proctor density	g cm^{-3}	–	1.7	1.45	1.76	1.57
Optimum water content (w_{opt} at D_{Pr})	$\%_{vol.}$	–	17	23.5	13.1	14.4
Total organic carbon (TOC)	% dw	76.6[b] ± 0.3	1.73 ± 0.1	6.2[c]	1.3[a]	5.8[c]
TOC/TN ratio	–	383[c]	11.5[c]	56.4[c]	13[c]	72.5[c]
pH		–	7.46 ± 0.2	7.58 ± 0.2	7.40 ± 0.02	7.63 ± 0.1
Electrical conductivity	μS cm^{-1}	–	295 ± 11.5	323 ± 3.5	231 ± 16	282 ± 14
C	% dw	77.8[b] ± 7.9	2.6 ± 0.1	3.4 ± 1.1	2.5 ± 0.9	5.6 ± 1.0
H	% dw	2[b] ± 0.3	0.5 ± 0.2	0.4 ± 0.06	0.4 ± 0.1	0.4 ± 0.02
N	% dw	0.2[b] ± 0.04	0.15 ± 0.005	0.11 ± 0.02	0.1 ± 0.03	0.08 ± 0.01
S	% dw	0.16[b] ± 0.05	0.07 ± 0.03	0.03 ± 0.01	0.03 ± 0.03	0.01 ± 0.01
O	% dw	16[b] ± 2.1	–	–	–	–

Silt loam = SiL; Loamy sand = LS; dw = dry weight; ± Standard Error (S.E.).
[a] Wieringermeer (Verseveld and Gebert, 2020).
[b] Sieved biochar.
[c] Calculated, BET surface area of biochar = 163 m^2 g^{-1} and biochar pore volume = 47.5 cm^3 g^{-1}.

3.1.1.2. Landfill cover soil with biochar. Adding biochar to Soil A increased the sand content and lowered the clay content without altering the soil texture class (Table 1). Similarly, the USDA texture class was the same for Soil C and Soil C + B despite the slight increase in silt and reduced clay and sand contents with biochar addition. For both soils, the 50 % mean diameter mass (d_{50}) obtained from the particle size distribution shifted by 12 % in the cumulative distribution curve from the biochar addition; thus, the volume mean diameter was not significantly modified (see Supplementary Information, Eqs. (S1) and (S2)).

Changes in the Proctor densities and optimum water contents were most prominent in soils with biochar amendment. Proctor density decreased with biochar, as shown in both Soil A + B and Soil C + B. The addition of biochar increased the total organic carbon contents, the TOC/TN ratio, and EC. The pH increased slightly with biochar. The most remarkable changes for all properties were shown in Soil C + B.

3.1.2. Compacted soils: bulk density, moisture content, and porosity

3.1.2.1. Landfill cover soil. Table 2 exhibits the typical physical properties (e.g., bulk density, total porosities, and moisture contents) of cover soils and soils amended with biochar at three levels of compaction (75 %, 85 %, and 95 % of the Proctor density). After testing the particle

Table 2
Density, moisture content, total porosity and air-filled porosity in compacted soils with and without biochar.

Compaction	Units	Soil A			Soil A + B			Soil C			Soil C + B		
	% Proctor	75	85	95	75	85	95	75	85	95	75	85	95
Bulk density	g dw cm^{-3}	1.27 ± 7 × 10^{-4}	1.44 ± 3 × 10^{-4}	1.61 ± 7 × 10^{-4}	1.09 ± 2 × 10^{-3}	1.23 ± 4 × 10^{-4}	1.38 ± 2 × 10^{-3}	1.31 ± 2 × 10^{-4}	1.48 ± 4 × 10^{-4}	1.65 ± 6 × 10^{-4}	1.18 ± 3 × 10^{-4}	1.33 ± 8 × 10^{-4}	1.49 ± 6 × 10^{-4}
Particle density	g dw cm^{-3}	2.65	2.65	2.65	2.48	2.48	2.48	2.65	2.65	2.65	2.48	2.48	2.48
Volume of solids	vol%	48	54.4	60.7	43.9	49.6	55.6	49.4	56	62.3	47.6	53.7	60.1
Volume of voids (Total porosity)	vol%	52 ± 0.03	45.6 ± 0.01	39.3 ± 0.03	56 ± 0.06	50.4 ± 0.02	44.3 ± 0.08	50.6 ± 0.01	44.1 ± 0.01	37.7 ± 0.02	52.4 ± 0.01	46.3 ± 0.03	39.9 ± 0.02
Volume of water	vol%	22.7	25.7	28.7	19.4	21.9	24.6	10.1	11.4	12.8	9.1	10.3	11.5
Matric potential	hPa	725	364	480	2200	2015	792	550	2538	4576	9492	9160	654
Water content	% dw	17.8 ± 0.01	17.8 ± 4 × 10^{-3}	17.80	17.8 ± 0.02	17.8 ± 0.01	17.8 ± 0.03	7.7 ± 2 × 10^{-3}	7.7 ± 2 × 10^{-3}	7.8 ± 0.02	7.7 ± 2 × 10^{-3}	7.7 ± 5 × 10^{-3}	7.7 ± 3 × 10^{-3}
Air-filled porosity (ε)	vol%	29.4 ± 0.03	20 ± 6.3	10.5 ± 5.8	36.6 ± 4.8	28.4 ± 4.4	19.7 ± 5.5	40.4 ± 2.5	32.7 ± 2.3	24.9 ± 3.1	43.2 ± 2.2	36 ± 2.1	28.4 ± 2.8
Number of samples (n)		5	5	7	5	7	6	5	9	5	5	9	5

dw = dry weight; ± Standard Error (S.E.); particle density of soil = 2.65 g dw cm^{-3}; particle density of biochar = 1.25 ± 0.08 g dw cm^{-3}, Soil A = silt loam; Soil A + B = silt loam with biochar; Soil C = loamy sand, Soil C + B = loamy sand with biochar, cubic-spline interpolation was employed to determine matric potentials >1000 hPa.

density of Soil A/Soil C in previous works (Holland and Gebert, 2020; Van Verseveld, 2018), a general average particle density of 2.65 g cm^{-3} was used to obtain the volume of solids and total pore volume (Blake, 2008). After compaction, the bulk densities in Soil C were slightly higher than in Soil A. However, the difference was small as the bulk densities corresponded to pre-defined levels of the Proctor density, which was quite similar (Table 1).

Total porosity at each compaction level was higher in the fine-grained Soil A than in Soil C and the air-filled porosity was significantly lower. In both soils, air-filled porosity decreased with compaction. Soil A, with higher proportion of finer particles (silt and clay, Table 1) and higher moisture contents, produced lower air-filled porosities than Soil C for all compaction levels. The gravimetric water content at a capillary pressure of 1000 hPa was significantly higher for fine-grained Soil A.

3.1.2.2. Landfill cover soil with biochar. Both soils with biochar addition decreased dry bulk density and increased total porosity (Table 2), which then increased air-filled porosity due to the low biochar particle density (1.25 g cm^{-3} ± 0.08 S.E.) and high biochar interstitial pore volumes (Fig. S2 in Supplementary Information), yielding higher soil porosities even when packed to a similar compaction force. The Brunauer-Emmett-Teller (BET) surface area was 163 m^2 g^{-1}, and the pore volume was 47.5 cm^3 g^{-1} per dry mass of biochar (Table 1 and Table S3 in Supplementary Information). The increase in total porosity and air-filled porosity upon biochar addition increased consecutively with the level of compaction in both soils (Supplementary Information, Fig. S3) reaching a maximum of 12.9 % compared to the original unamended soil (highest compaction level in fine-grained Soil A). The gain in total porosity and, given that the water content was not changed, the air-filled porosity was highest in the finely textured Soil A at all compaction levels. In this soil, biochar amendment increased air-filled porosity by a maximum of 87 % compared to the unamended soil.

3.1.3. Pore size distribution and soil water retention curves (SWRC)

The impact of biochar amendment on the soil water retention curve is presented in Supplementary Information, Fig. S4. The volumetric water contents at saturation declined with increasing compaction, similar to the porosity results in Table 2, as the void spaces available for water storage diminished from compaction. At the same water content, biochar-amended soils had slightly higher capillary pressures, thus dryer than the non-biochar-amended soils for both soils between 100 and 1000 hPa for all samples except in Soil A compacted to 75 %. At higher capillary pressures (>10^4 hPa), the curves of the amended and unamended soils converged, and the water content improvements were not observed. The most significant water content improvements were shown in the lower capillary pressure ranges (<1000 hPa). There is a data gap between 1000 and 10^4 hPa due to limitations in the instruments employed, where the Hyprop™ has a maximum capillary pressure measurable to ~1000 hPa and the minimum pressure of ~10,000 hPa for WP4C™ dewpoint potentiometer. Nevertheless, the SWRC were used to estimate pore size distributions using Eqs. (8) and (9) and illustrated in Fig. 1.

3.1.3.1. Landfill cover soil. Increasing compaction lowered the total porosity as expected (Table 2), and thus, the saturated volumetric water contents for both Soil A and Soil C decreased (Supplementary Information, Fig. S4). However, pore size distribution fractions showed a different trend with increasing compaction for Soil A (Fig. 1). Soil A compacted at 75 % Proctor density had lower pore volumes than 85 % compaction at P_c < 60 hPa, and the 95 % compaction had the lowest pore volume percentage. Larger pores (macropores) in 75 % compaction were more susceptible to pore reduction upon compaction than at 85 % D_{Pr} in Soil A and small pore volumes (e.g., micropores) have the smallest impact on compaction (Sleutel et al., 2012). Soil C decreased pore

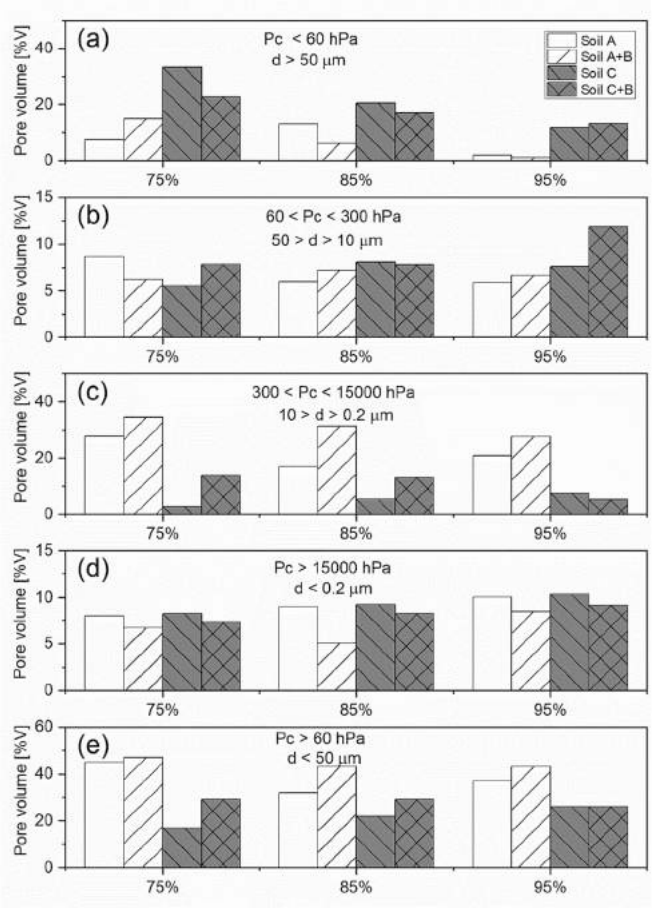

Fig. 1. Pore volume distribution histograms of Soil A and Soil C with and without biochar at different compaction levels at (a) capillary pressures (P_c) < 60 hPa, (b) 60 < P_c < 300 hPa, (c) 300 < P_c < 15,000 hPa, (d) P_c > 15,000 hPa, and (e) P_c > 60 hPa.

volume sizes with increasing compaction at P_c < 60 hPa, consistent with the total porosity trends. The highest share of pores for coarse-grained Soil C was in the P_c < 60 hPa region (32 to 66 % of the total porosity).

There was no clear trend in the share of pore volumes to compaction levels beyond the saturation region for all the samples, particularly after air started entering the compacted soils beyond the air-entry pressure. The highest pore volume in the 60 < P_c < 300 hPa region was measured on 75 % compaction for Soil A, whereas the lowest pore volumes were observed on 75 % compaction for Soil C. The highest percentage of pores was found in the 300 < P_c < 15,000 hPa region for Soil A, ranging from 38 to 54 % of the total porosity, compared to 6 to 21 % of the total pores in coarse-grained Soil C. At P_c > 15,000 hPa, the percentage of pores ranged between 15 and 26 % for both Soil A and Soil C for all compaction levels.

3.1.3.2. Landfill cover soil with biochar. Biochar amendment increased the total porosity of Soil A for all compaction levels by 7 % to 12 % and by 4 % to 6 % between Soil C and Soil C + B (Table 2 and Fig. S3). Biochar addition increased field capacity (P_c > 60 hPa) and hence the maximum amount of water that can be stored against gravity in both soils at all compactions, except for the 95 % level in coarse-grained Soil C + B (Fig. 1). For Soil C at 95 % compaction level (P_c > 60 hPa), the impact of biochar was negligible. Biochar showed no improvement of soil pores at P_c < 60 hPa (d > 50 µm) except at 75 % compaction level in Soil A + B (66 % increase in d > 50 µm pore diameter). Biochar addition most profoundly increased the pore diameter at 10 > d > 0.2 µm (equivalent to 300 < Pc < 15,000 hPa) with all compaction levels.

Biochar showed the highest pore volume improvement at $300 < P_c < 15{,}000$ hPa for all compaction levels (except for Soil C + B at 95 % compaction): the increase ranged from 21 to 59 % for Soil A + B and 83 to 133 % in Soil C + B. In Soil A + B, this pore class ($10 > d > 0.2$ μm) represented ~62 % of the total pores, and in Soil C + B, the pores represented 13–28 % of the total pores. Biochar amendment lowered pore volumes at $P_c > 15{,}000$ hPa ($d < 0.2$ μm at $P_c > 15{,}000$ hPa) for both Soil A and Soil C for all compaction levels.

3.2. Methane oxidation

3.2.1. Methane oxidation in loose soil (pre-incubation)

All samples were pre-incubated for ~105 d to maximize the methane removal rates by activating the methane-oxidizing bacteria and providing methanotrophic communities the time to proliferate to their respective maximum level. Landfill cover soils with a different history of CH_4 exposure will have distinct methane oxidation rates. Therefore, pre-incubating the soils with CH_4 to reach a maximum capacity serves as a way to establish a steady-state condition for both soil types to compare the soils with two different CH_4 exposure histories. Thus, the CH_4 oxidation rates observed after compaction of loose soil should reflect only a response to changes in porosity and gas transport properties at a constant water content. Fig. 2a and b illustrate the methane oxidation rates during the pre-incubation stages of loose soils and the buildup of methane oxidation capacity over time.

The oxidation rates were initially higher for Soil A/Soil A + B at 17.8 % gravimetric water content than Soil C/Soil C + B mixtures (5.9 % gravimetric water content from 0 to 69 d of pre-incubation time) and increasing markedly, suggesting an already active soil conducive to methane oxidation. Because the methane oxidation rates were slow in Soil C/Soil C + B, the gravimetric water contents were increased to 7.7 % (w/dw) on 70 d of the pre-incubation study. After 71 d of incubation, Soil C/Soil C + B started exponentially increasing methane oxidation rates, and the gravimetric water contents of 7.7 % (w/dw) were maintained in the Soil C/C + B mixtures for the remainder of the study.

At the end of the pre-incubation period between 99 and 105 d of methane exposure, the rates calculated in dry mass were 1117 ± 45 mg CH_4 kg_{dw}^{-1} d^{-1} for Soil A, 946 ± 66 mg CH_4 kg_{dw}^{-1} d^{-1} for Soil A + B, 861 ± 63 mg CH_4 kg_{dw}^{-1} d^{-1} for Soil C, and 820 ± 64 mg CH_4 kg_{dw}^{-1} d^{-1} for Soil C + B. The differences between Soil A and Soil C, and Soil A and Soil C + B were statistically significant ($P < 0.05$). The difference between Soil A + B and Soil C + B was statistically insignificant ($P > 0.05$). Despite the 16.5 % difference between Soil A and Soil A + B, and the 5 % difference between Soil C and Soil C + B of the mean methane oxidation rates, these differences were statistically insignificant ($P > 0.05$), and the initial methane oxidation rates were indistinguishable between the natural soils and the biochar-amended soils.

3.2.2. Methane oxidation in compacted soil

After compacting the soils into the ~100 cm^3 steel cores and exposing them to methane in individual jars, the methane oxidation rate continued to increase with progressive duration of incubation for some samples, excluding Soil A + B for all compaction levels, and Soil A and Soil C at 95 % Proctor compaction (compare average rates for 1–3 phases with average rates for 18–20 phases, Fig. 2c).

3.2.2.1. Landfill cover soil. Methane oxidation rates were higher in Soil A at 75 % and 85 % compaction levels within the first three phases of incubation within three days after sample compaction (Fig. 2c). The oxidation rates estimated from the dry soil mass increased from 1117 mg CH_4 kg_{dw}^{-1} d^{-1} during pre-incubation (Fig. 2a & 2b) to 1312 mg CH_4 kg_{dw}^{-1} d^{-1} for 75 % compaction (Fig. 2c) and to 1282 mg CH_4 kg_{dw}^{-1} d^{-1} for 85 % compaction (Fig. 2c). At 95 % of the Proctor density, the methane oxidation rates in Soil A plummeted by ~83.5 % from the pre-incubation rate to ~185 mg CH_4 kg_{dw}^{-1} d^{-1}. With more prolonged incubation, the methane oxidation rates increased in Soil A as shown in the 18–20 phases, except when Soil A was compacted to a 95 % level that decreased to approximately 33.8 mg CH_4 kg_{dw}^{-1} d^{-1}. Soils with higher clay and silt contents were more susceptible to compaction and showed a more significant change in soil pore structures than sandy soils (Gupta et al., 1989). Hence, the same effect on Soil C was not observed for the 95 % compaction level.

The methane oxidation performance in coarse Soil C varied less in comparison to fine Soil A. The methane oxidation rates measured within the first three phases after compaction were similar to the loose soils for all three compaction levels. There was no change in oxidation rates initially after compacting the samples to three different levels. The oxidation rates ranged from 840 ± 46 to 954 ± 67 mg CH_4 kg_{dw}^{-1} d^{-1} for all three compactions and were statistically insignificant with $p > 0.05$ for all compacted samples, including the Soil C oxidation rates at pre-incubation. However, for the final three phases of incubation, the methane oxidation rates in Soil C significantly increased in samples compacted at levels 75 % and 85 %, similar to Soil A. The dense compaction at 95 % in coarse Soil C performed better than Soil A with a mean oxidation rate of 1167 ± 25 mg CH_4 kg_{dw}^{-1} d^{-1}, but the oxidation rates were statistically insignificant ($p > 0.05$) to the rates of the loose soil in Soil C, indicating that rates did not increase drastically from the loose condition.

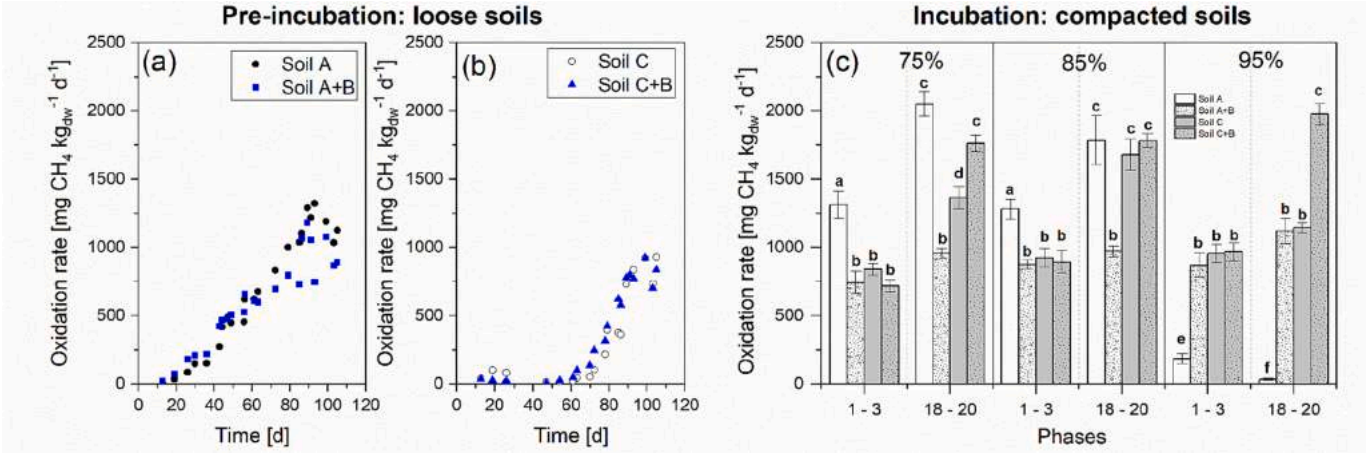

Fig. 2. Mean methane oxidation rates during pre-incubation (loose soil, left) and of compacted samples (75 %, 85 %, 95 % Proctor density, right) over time of incubation, with (closed symbols) and without (open symbols) biochar. Phase = one complete cycle of oxidizing 10 vol% CH_4. Incubation time for Phases 1–3 was 0 to 0.22 d and 58 to 73 days for Phases 18–20. Error bars = standard error. Letters denote significant differences between samples ($p < 0.05$).

3.2.2.2. Landfill cover soil with biochar. Biochar addition decreased methane oxidation rates at 18–20 phases in fine-grained Soil A at 75 % and 85 % Proctor by 55 % and 37.5 %, respectively. Only at the 95 % compaction level, biochar prevented the collapse of methane oxidation in Soil A, maintaining rates similar to Soil A at pre-incubation. During 1–3 phases of soil incubation in Soil A + B, the methane oxidation rates were similar between all compaction levels, and the rates prevailed until the end of the experiment. In Soil C, rates were similar with and without biochar in the beginning and strongly increased throughout the experiment at 75 % and 85 % Proctor compaction. Long-term improvement in CH_4 oxidation rate is seen for both Soil A and Soil C with biochar addition at the highest compaction level.

3.2.3. Gas diffusivity of soils and relation to CH_4 oxidation

Normalized gas diffusivity (D_p/D_o) increased linearly with lower soil density and increased air-filled porosity (Fig. 3a). Soil A mixtures had lower gas diffusivity than Soil C for all compaction level equivalents (Table 3). Biochar addition enhanced gas diffusivity by 19–48 % in Soil A and 23–72 % in Soil C for all compaction levels (Figs. 3a & Table 3).

The methane oxidation rates for the mixtures show that the highest peak rates were observed in Soil A at 75 % compaction level, surpassing the rates of all biochar/soil combined mixtures (Fig. 3b). The lowest oxidation rates were found in Soil A at 95 % compaction level in the last three phases of incubation. Compaction concomitantly reduced methane oxidation in Soil A, but a different trend was observed in Soil C, where the highest methane oxidation was found in 85 % compaction level, and the lowest rate was observed in 95 % compaction, but the rate ranged between 1366 and 1680 mg kg_{dw}^{-1} d^{-1}. Adding biochar to soils did not improve methane oxidation rates in Soil A despite having higher oxygen transport than the original soil except in 95 % compaction. Soil C followed a different pattern than Soil A, where biochar improved the CH_4 oxidation rates the most in Soil C + B at 95 % compaction. Data suggest that the methane oxidation rates elevated progressively in Soil A (Fig. 2b) from the initial phases to the final phases of incubation in the 75 % and 85 % D_{Pr} compacted soils. However, biochar application disrupted methanotrophic activity as the methane oxidation rates stagnated in Soil A for the two compaction levels but were not inhibited. Compaction and biochar addition improved CH_4 oxidation in coarser soils with variable pore volume distribution (Figs. 1 and 3b) than in Soil A, indicating that biochars did not have toxic properties, and pore size classes may have an important role in microbial activity (Sleutel et al., 2012). The decreased CH_4 oxidation rates in Soil A + B under 75 % and 85 % compaction levels are soil-specific and could be attributed to the reduction in certain pore size classes from compaction, biochar breakage, and the accumulation of water in soil micropores during incubation. Despite the clear inverse relationship between gas diffusivity and soil compaction, methane oxidation rates varied only minimally with compaction, except for the collapse in fine Soil A at 95 % of the Proctor density (Fig. 3b). Coarse Soil C + B maintained oxidation rates twice as high as fine Soil A + B at all compaction levels. Biochar amendment in fine Soil A almost halved the methane oxidation rate, except for the highest compaction.

Biochar amendment improved specific diffusivity at all compaction levels in the coarse Soil C but only at the 75 % compaction level in fine-grained Soil A (Table 3). Based on the potential flux, coarse Soil C mixtures had higher O_2 transport with higher expected J_{CH4} potential flux than finer Soil A. Adding biochar enhanced the J_{O2} and J_{CH4} potential flux for all sample types, with the highest potential flux observed in the lowest compacted coarse soil. However, the potential oxygen flux represents the maximum oxygen transport in the soil, not the actual oxygen flux. The actual oxygen flux trended contrary to the potential oxygen flux. In unamended soils, finer Soil A had the highest oxygen flux compared to the coarse soil, and the oxygen transport increased with increasing compaction levels for most samples. Furthermore, the addition of biochar decreased the oxygen flux for both soil types.

Fig. 4 illustrates the sample depths at which diffusive O_2 supply would deplete and start to limit CH_4 oxidation based on Fick's law. In a simplified approach, it was assumed that the entire CH_4 oxidation (one mol of CH_4) would occur in a specific depth and that the required O_2 flux (two moles of O_2) would have to reach this depth using the measured methane oxidation rates of compacted samples as an indicator of the actual oxygen flux. Adding biochar and/or using coarse soil will enhance O_2 penetrable depth, thus showing higher oxygen intrusion depth in coarse Soil C than in the finer Soil A. Adding biochar to a finer soil enhanced oxygen infiltration depth but remained below 0.6 m for all compaction levels. The highest oxygen intrusion depths were in coarse Soil C + B. In line with decreasing effective diffusivity (coefficient D_p), increasing compaction level decreased the depth reachable by O_2.

3.3. Composition of the methanotrophic population

A total of 1045 species were identified, of which 18 were methanotrophic species (also see Fig. S5 in Supplementary Information). All samples, including the loose soil at the end of the pre-incubation stage, Soil A and C with and without biochar, showed a strong dominance of Type II species, namely *Methylocystis*, followed by *Methylocella* and, in most samples by *Methylosinus*. Apparent differences between the communities' response to compaction and biochar amendment were seen; however, no relation between abundance or community composition and observed CH_4 oxidation rates was found (Fig. 5).

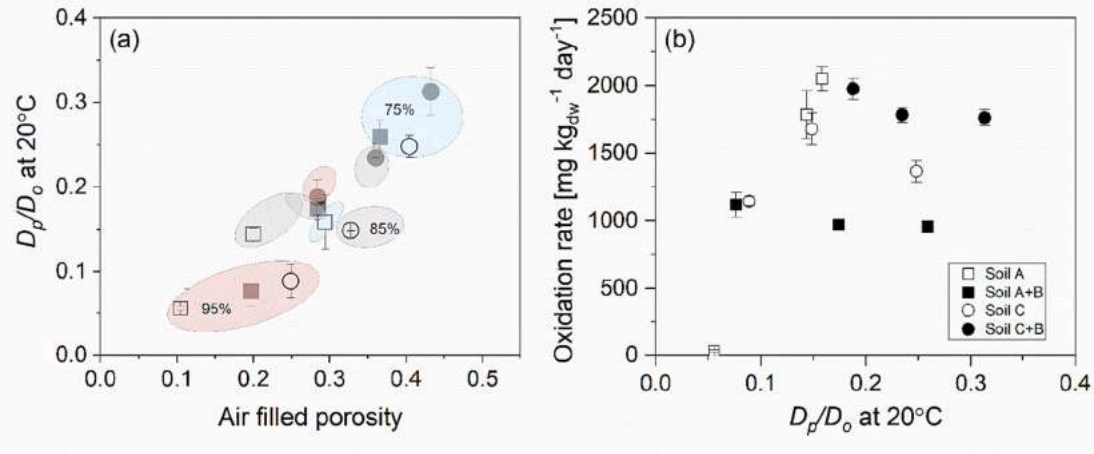

Fig. 3. Gas diffusivity of compacted samples with and without biochar: (a) compared against porosity where the colored ellipses indicate compaction levels (blue = 75 %, grey = 85 %, red = 95 % compaction), and (b) compared with CH_4 oxidation rates averaged over phases 18–20 (see also Fig. 2c).

Table 3
Gas diffusivity and gas transport properties.

Compaction	Units	Soil A			Soil A + B			Soil C			Soil C + B		
	% Proctor	75	85	95	75	85	95	75	85	95	75	85	95
D_p/D_o	m^2s^{-1}	0.16	0.14	0.06	0.26	0.17	0.08	0.25	0.15	0.09	0.31	0.23	0.19
(S.E.)	±	0.03	0.01	0.00	0.02	0.01	0.02	0.01	0.00	0.02	0.03	0.00	0.02
D_p	m^2s^{-1}	3.3×10^{-6}	3×10^{-6}	1.2×10^{-6}	5.4×10^{-6}	3.7×10^{-6}	1.6×10^{-6}	5.2×10^{-6}	3.9×10^{-6}	1.9×10^{-6}	6.6×10^{-6}	4.9×10^{-6}	3.9×10^{-6}
(S.E.)	±	6.7×10^{-7}	8.8×10^{-8}	4.2×10^{-8}	4.2×10^{-7}	1.7×10^{-7}	3.9×10^{-7}	2.8×10^{-7}	4.5×10^{-7}	4.2×10^{-7}	6.0×10^{-7}	8.3×10^{-9}	4.4×10^{-7}
Specific diffusivity (D_p/ε)	m^2s^{-1}	1.1×10^{-7}	1.5×10^{-7}	1.1×10^{-7}	1.5×10^{-7}	1.3×10^{-7}	8.1×10^{-8}	1.3×10^{-7}	1.2×10^{-7}	7.5×10^{-8}	1.5×10^{-7}	1.4×10^{-7}	1.4×10^{-7}
J_{O2} potential flux	g O_2 m^{-2} d^{-1}	3422	3090	1205	5595	3760	1657	5359	3209	1917	6757	5065	4056
$J_{O2,exp}$ actual flux[a]	g O_2 m^{-2} d^{-1}	261	257	5	104	120	155	179	249	189	208	237	294
J_{CH4} potential flux	g CH_4 m^{-2} d^{-1}	856	773	301	1399	940	414	1340	802	479	1689	1266	1014
J_{CH4} oxidized (avg. of phases 18–20)	g CH_4 m^{-2} d^{-1}	65.1	64.3	1.3	26.1	29.9	38.7	44.7	62.2	47.2	51.9	59.3	73.6

[a] J_{O2} actual flux was obtained by calculating the flux using the last three phases of the CH_4 oxidation rates during incubation of compacted soils and the bulk density of the compacted samples (Eqs. (5) & (7)), D_p/D_o = gas diffusivity, D_p = gas diffusion, ε = air-filled porosity, J = gas flux, S.E. = Standard Error.

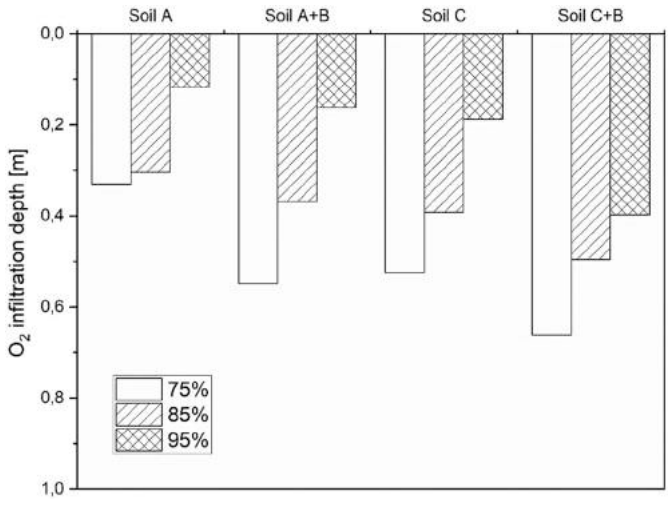

Fig. 4. Oxygen infiltration depth at an averaged methane load of 2.41 ± 0.01 mg CH_4 per cm^2.

3.3.1. Landfill cover soil

In loose soil conditions, methanotrophs represented 6.5 % of the hybridization product in Soil A and 6 % in Soil C. The most abundant methanotrophic species was *Methylocystis*, representing 2.9 % of the relative abundance of the microbial composition in Soil A and 2.4 % in Soil C. The second and the third most abundant methanotrophic species were *Methylocella* and *Methylosinus* for all sample types. Type II methanotrophs *Methylocystis*, *Methelocella*, and *Methylosinus* represented 44 %, 14 %, and 10 % of relative abundance of the total methanotrophs in loose soils for Soil A and 41 %, 11 %, and 7 % for Soil C, respectively. Representatives of Type I methanotrophs consisted of *Methylomicrobium* and *Methylomonas*. With these two species combined, Soil A had 0.21 % (0.14 % *Methylomicrobium* and 0.07 % *Methylomonas*) and Soil C had 1.7 % (1 % *Methylomicrobium* and 0.7 % *Methylomonas*) Type I methanotrophs from the relative abundance of the total microbial composition, representing 3.1 % and 27.7 % of the total methanotrophs in Soil A and Soil C, respectively.

After compaction and continued incubation, the relative abundance of methanotrophs increased slightly in both Soil A and Soil C for all compaction levels. Similar to the loose soils, Type II methanotrophs (*Methylocystis*, *Methylocella*, *Methylosinus*) were the dominant methanotrophs in both Soil A and Soil C, with a slightly higher abundance in Soil A (ranged ~7–9 % abundance) than in Soil C (ranged 5–6 % abundance) for all compaction levels. *Methylocystis* represented the most abundant genus in all compacted samples. Type I methanotrophs represented <1 % of the total abundance for both soil types at all compaction levels.

3.3.2. Landfill cover soil with biochar

In the biochar-amended and compacted soils, MOB abundance did not change in fine-grained Soil A (Fig. 5a), consistent with the methane oxidation rates (Fig. 3), possibly due to the differences in soil texture. The response could be unpredictable since there was no correlation between the pore size distribution, soil moisture characteristics, gas diffusivity, O_2 availability, and compaction on methanotrophic community composition. Biochar markedly improved coarsely-grained Soil C (Fig. 5b). Here, relative abundance of methanotrophs doubled upon biochar amendment at all compaction levels and in the loose soil as the biochar primarily enhanced pore structure in coarse sandy soil and diversified the pore size classes. *Methylocystis* benefited the most from biochar amendment, with abundances increasing by over a factor of three. In coarsely-grained Soil C, biochar addition increased the relative abundance of Type II species to 90 % of total methanotrophs prior to soil compaction, while Type II methanotrophs did not increase upon biochar amendment in Soil A. In the loose, pre-incubated soil, Type I abundance was similar in Soil A with and without biochar (~2 % of the total species), while biochar amendment significantly reduced Type I abundance in Soil C from ~35 % to ~8 % of the total methanotrophs. Compaction reduced the share of Type I methanotrophs in Soil C even further to <6 % of the total methanotrophs and ~ 1 % of all species. While, as described, the relative abundance of the microbial composition enormously increased upon biochar amendment in coarsely grained Soil C, but no systematic differences between the compaction levels were seen.

4. Discussion

This study investigated if methane oxidation rates and methanotrophic community composition of two landfill cover soils at different compaction levels could be enhanced by adding fir-wood biochar through the hypothesized beneficial effects of the increase in air-filled porosity and water retention capacity. Biochars are believed to enhance soil properties relevant to improve methane oxidation, however, the beneficial effects were different for the two landfill cover soils employed in this study.

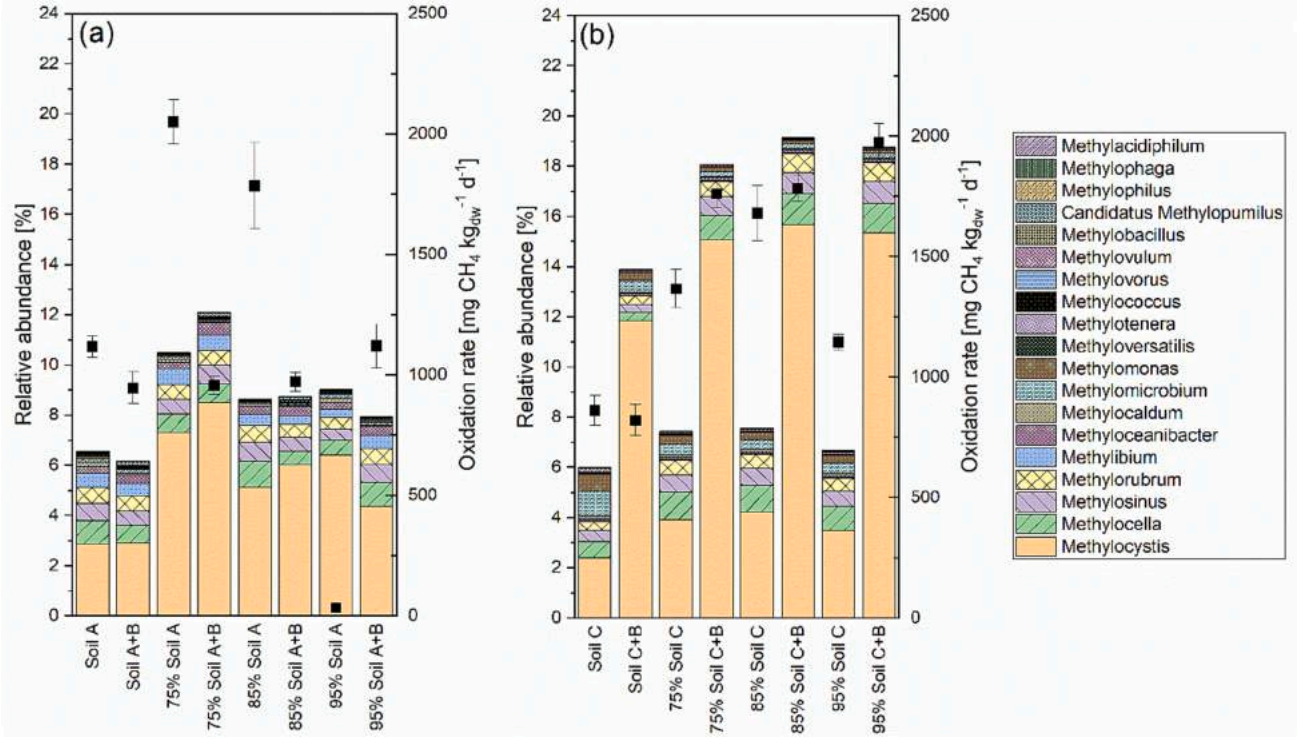

Fig. 5. Composition of the methanotrophic communities and methane oxidation rates. (a) Soil A (Braambergen soil) and Soil A + B (Braambergen soil +6 % *w*/w biochar); (b) Soil C (Wieringermeer soil) and Soil C + B (Wieringermeer soil +6 % w/w biochar). Left two columns in each figure represent the loose soil at the end of the pre-incubation period. 75 %, 85 % and 95 % signifies the compaction level of the sample packings.

4.1. Soil compaction, diffusivity, pore size characteristics and water retention

Compaction reduced air-filled porosity and gas diffusivity in both soils (Tables 2 & 3), with relative change being soil-dependent. Coarse Soil A in this study showed lower changes than compaction-susceptible finer soil under the same compaction regime (Gebhardt et al., 2009). At all compaction levels, air-filled porosity and gas diffusion coefficients were higher in coarse-grained soil than in finer-grained soil and were increased by the addition of biochar (Table 2). The highest diffusion coefficients were observed in the coarse Soil C mixtures with biochar. However, the largest relative increases in total porosity and air-filled porosity and diffusivity were observed for the fine-textured Soil A. The results corroborated with Amoakwah et al. (2017) and Sun et al. (2013), who observed that increases in diffusivity corresponded to increased air-filled porosity resulting from biochar addition (Amoakwah et al., 2017; Sun et al., 2013).

However, compaction and biochar amendment on soils distorted pore size distribution. Of all pores size classes, the coarse pores >50 μm (equivalent capillary pressure of P_c < 60 hPa, Fig. 1a) were reduced mostly by compaction, shifting the pore size distribution towards the smaller diameter, as also reported previously (Gebhardt et al., 2009; Verseveld and Gebert, 2020; Wickramarachchi et al., 2011). Biochar amendment decreased the share of coarse pores >50 μm (Fig. 1a) at all compaction levels (except for 75 % D_{Pr} in Soil A). Biochar significantly increased medium size pores (0.2–10 μm, Fig. 1c), except for the 95 % compaction level in fine Soil A, and always reduced the share of pores <0.2 μm (Fig. 1d). Changes in the share of fine coarse pores at 10–50 μm were equivocal, as clear trends did not emerge. In Soil C and Soil C + B, the pore size distributions were both diverse and varied, providing sufficient pore spaces in all pore classes, whereas >40 % of pores were in P_c > 60 hPa region for Soil A and Soil A + B (Fig. 1). Interestingly, soils with pores distributed more evenly between the varying pore fractions from 0 to >15,000 hPa performed better than soils with only one pore fraction dominating. Despite the slight reduction in pore volumes at P_c < 60 hPa and P_c > 15,000 hPa for all biochar-amended Soil C, the methane oxidation rates were, therefore, higher with biochar amendment.

Compaction can fracture biochar particles, producing smaller particles that decrease pore size (Lamprinakos and Manahiloh, 2019) as fine particles are packed firmly between the larger pores. Compaction of biochar-amended soil will change the pore size distribution, and this effect would likely change saturated hydraulic conductivity and advective gas transport at larger scales, which both are strongly affected by the pore diameter (Hagen, 1839; Poiseuille, 1840; Stokes, 1845). Spokas and Bogner (2011) observed that the optimum methane oxidation condition could be at capillary pressure of ~500 hPa, and the oxidation rate can decrease by ~50 % when the soil moisture becomes drier than 7000 hPa (Spokas and Bogner, 2011). Therefore, if the pore volume at ~500 hPa is enhanced, an increase in methane oxidation is expected. In the study, the soil moisture potential was not set at 500 hPa to normalize the soil variability to achieve the optimal methanotrophic activity, but at 1000 hPa (a lower moisture content) to ensure that water logging did not occur, and sufficient moisture was available for the MOB. However, water enhancement may occur in smaller pore fractions, and water evaporation may occur in larger pores, possibly affecting methane oxidation. It was observed that biochars increased pore volumes at P_c = 500 hPa for all samples except in Soil C + B at 85 % and 95 % compaction (Supplementary Information, Table S5), but the matric potential mostly increased in soils with biochar amendment at the same gravimetric water contents (Table 2). Furthermore, adding biochar reduced the pores above 15,000 hPa matric potential, which can be easily filled with water that can decrease methane oxidation rates. The reduced oxidation rates in Soil A + B at 75 % and 85 % Proctor compactions may have occurred due to water accumulation in biochar-concentrated regions where the gravimetric water contents can increase by four times the original amount (Yargicoglu and Reddy, 2017b), locally reducing the O_2 and CH_4 flux, corroborated by increased share of

medium-sized pores (0.2–10 μm, Fig. 1c) despite keeping the gravimetric water contents constant.

Compaction significantly increased the volumetric water content, while biochar amendment reduced the volumetric water content, increasing the matric potential (Table 2). By changing the pore size distribution of soils, biochar amendment led to a redistribution of moisture across different pore sizes (Fig. 1). In finer soil, depending on the type of biochar, water retention can be decreased if the internal porosity of biochar gets clogged and/or the biochar specific surface areas are lower than soils (Yi et al., 2020), thus controlling CH_4 oxidation, especially in cases where soils become too dry or when a larger proportion of small diameter pores (e.g., $d < 0.2$ μm) become filled with water. Methane oxidation will be more susceptible to water in fine soils than in coarse soils (Huber-Humer et al., 2008) as capillary forces are higher and large, and drainable pores are less abundant.

At high compaction, the increased air-filled porosity from 10.5 to 19.7%$_{vol}$ explains the positive effect of biochar on CH_4 oxidation when air-filled porosity is in the region of diminished pore connectivity (~10%$_{vol}$) (Gebert et al., 2011; Moldrup et al., 2001). In these cases, biochar addition improved air-filled porosity and pore connectivity, preventing the collapse of CH_4 oxidation rates due to the development of O_2-depleted sites in the soil (Gebert et al., 2016; Horn and Smucker, 2005). In coarse Soil C + B, biochar mostly improved long-term CH_4 oxidation rates, with the greatest impact found at the highest level of compaction, even though biochar lowered the volumetric water contents at the same gravimetric water content (Table 2). The highest oxidation rates were observed on coarse Soil C + B at 95 % compaction (Fig. 2c).

Against expectation, enhancement of air-filled porosity and gas diffusivity from biochar addition (Fig. 3) did not improve methane oxidation rates in the fine-grained soil. Instead, biochar benefitted the oxidation rates in the coarse-grained soil. The moisture content may influence the methane oxidation rate, as at constant gravimetric water content, biochar-amended soil had a lower volumetric water content, hence a higher matric potential (capillary pressure) than the control soil. A major limitation of the study was not accounting for the variation of moisture contents in the compacted biochar-amended soils and the implications on methane oxidation and methanotrophs. The moisture contents were set constant to examine the changes in methane oxidation rates and methanotrophs' adaptability when porosity is altered, influencing gas transport.

Continued exposure of methane to loose soils during pre-incubation promoted methanotrophic communities to adapt to the higher methane exposure, and the incubation of compacted samples led to a sustained increase in CH_4 oxidation rates (Figs. 2a – 2c) reaching the values >2000 mg CH_4 kg_{DW}^{-1} d^{-1} (equals 83 μg g_{dw}^{-1} h^{-1}), illustrating the importance of methane exposure to the substrate before assessing the suitability of a soil for use in methane oxidation systems (Röwer et al., 2011; Spokas and Bogner, 2011). Methane pre-incubation normalized all four soil types (Soil A and C, with and without biochar) to similar oxidation rates (Fig. 2a and b), indicating that biochar amendment did not significantly affect CH_4 oxidation in the loose soils. Methane adsorption can occur in porous carbon materials affecting methane oxidation rates, but this effect was not observed, and the biochar's specific surface area was too low for this process to dominate (Memetova et al., 2022; Sadasivam and Reddy, 2015). The oxidation rates exceeded the previously reported values from batch testing at similar temperatures, which ranged 43 to 1133 mg CH_4 kg_{DW}^{-1} d^{-1} (Scheutz et al., 2009; Spokas and Bogner, 2011).

In the compaction experiment, CH_4 oxidation rates were not systematically affected by the reduced air-filled porosity and diffusivity induced by compaction (Fig. 3), except for fine-grained Soil A at the highest compaction level (95 % D_{Pr}) that showed CH_4 oxidation plummeting to approximately 33.8 mg CH_4 kg_{dw}^{-1} d^{-1}. This means that higher air-filled porosity related to lower compaction or biochar addition did not govern methane oxidation unless biochar supported the collapse of pore structures in the soil media when air-filled porosity reduced to <10 % at a 95 % compaction level. CH_4 oxidation rates remained relatively constant for all compaction levels at different diffusivities when biochar was added to both soils (Figs. 3b). Coarse soils, both with and without biochar, mostly exhibited higher methane oxidation rates and oxygen flux with increasing compaction despite having lower diffusivity with higher density.

It is noteworthy that in all samples, the potential diffusive O_2 flux greatly exceeded the measured and the calculated O_2 flux needed to facilitate the observed CH_4 oxidation rates. This indicates that O_2 diffusion did not limit the methane oxidation process in the experimental setup with shallow soil specimens (total height of 5 cm), resulting in high O_2 concentration gradients (Table 3). Furthermore, methane emissions may exceed if the CH_4%$_{vol}$ treatable is higher than the volume of soil with active methanotrophs (Yargicoglu and Reddy, 2017b) since the addition of biochar to soil increased not only the potential O_2 flux but also the potential CH_4 flux (Table 3). Design of high-performing methane oxidation systems should avoid limiting the process to the upper crust of the soil. Calculating the potential depth of diffusive O_2 ingress (Fig. 4), shows that compaction significantly decreases the depth to which O_2 can penetrate and that biochar mitigates the adverse effect of compaction. Further, in line with the lower diffusion coefficients, the available depth is higher in coarse-grained soils than in fine-grained soils that are also more susceptible to mechanical stresses (Gebhardt et al., 2009; Lamprinakos and Manahiloh, 2019).

4.2. Composition of the methanotrophic community

All samples were dominated by Type II methanotrophs. However, the response of community composition in the two soils to biochar addition was quite different. Application of biochar did not increase the total methanotrophic abundance in finer-grained Soil A but more than doubled the abundance in all samples of coarse-grained Soil C, including the loose soil at the end of pre-incubation (Fig. 5). An increase in total abundance could entirely be attributed to an increase in the relative abundance of the genus *Methylocystis*. However, this did not reflect in increased CH_4 oxidation rates. Very clearly, abundance and CH_4 oxidation rates were unrelated over the entire sample set of loose and compacted soils, with and without biochar, as reported in other studies from natural environments (Hunt et al., 2013; Nagler et al., 2021). Methanotrophic abundance also showed no relation to compaction, in either of the soils since the increase in *Methylocystis* upon biochar amendment in coarse Soil C was neither related to oxidation rates nor compaction and hence volumetric water content and air-filled porosity. It is suspected that *Methylocystis* benefitted from, for example, biochar-associated nutritional elements, additional surface area for colonization or increased moisture content around biochar particles in coarse soil.

The proliferation of Type II methanotrophs is favored by high levels of methane, low levels of O_2, and limited concentrations of nitrogen and or copper (Hanson and Hanson, 1996). The Type II genus *Methylocystis* was the most abundant in all samples from both soils, with and without biochar, followed by *Methlyocella* and *Methylosinus*. Type II dominance and high abundance of *Methylocystis* and *Methylosinus* were also found in studies by Gebert et al. (2009) for cover soils from old landfills and by Huang et al. (2019) in a sandy loam landfill cover soils amended with biochar, and in biofilters used for the biological treatment of landfill gas (Gebert et al., 2009; Huang et al., 2019).

Methylocystis species can consume high levels of methane from landfills and low concentrations of atmospheric methane (Bao et al., 2014; Huber-Humer et al., 2008). Type II methanotrophs are mesophilic and neutrophilic microorganisms that can fix nitrogen (Bodelier, 2011) and grow between 15 °C to 37 °C with an optimum temperature of 30–35 °C (Jung et al., 2020). *Methylocystis* is considered a versatile genus, able to adapt to diverse environments under stress and to survive under fluctuating methane concentrations (Jung et al., 2020).

Yargicoglu and Reddy (2017a) found that the Type I methanotrophs *Methylomonas* and *Crenothrix* dominated in landfill cover soils, with the highest population found in samples without biochar (Yargicoglu and Reddy, 2017a). However, these soils were characterized by low permeability with low oxidation rates. Also, here, an impact of CH_4 exposure to the substrate in laboratory incubations on methane oxidation was suspected. Type I MOB are dominant in environments in which methane is limited and high nitrogen levels prevail (Hanson and Hanson, 1996). Type I methanotrophs were detected in this study, however, the relative abundance of the microbial composition was below 2 %.

5. Conclusions

The study investigated the impact of adding fir-wood biochar to active landfill cover soils employed at two different Dutch landfills with moderate oceanic climates. The purpose of the study was to understand the underlying mechanisms involved in methane oxidation and assess the feasibility of implementing biochar on a larger scale through batch tests to understand the application of fir-wood biochar changing the physical landfill cover soil properties affecting methane oxidation and methanotrophic population at 75 %, 85 %, and 95 % compaction levels.

Waste management operators and researchers are interested in utilizing biochar to reduce methane emissions, and batch testing serves as an inexpensive and rapid means to determine if applying fir-wood biochar to landfill soil covers is optimal for their landfills. The batch tests provide essential knowledge of soil properties and behaviors of methanotrophs under various compaction levels, enabling operators to evaluate and identify limitations and make necessary adjustments to reduce landfill CH_4 emissions using biochar before field-scale implementation. Thus, tests were conducted to examine the influence of biochar on methane oxidation kinetics in relation to soil textures, porosity, and gas diffusivity at a constant moisture content under three levels of compaction. Based on the results, the following conclusions can be drawn:

- CH_4 oxidation rates are heavily driven by previous methane exposures. Continued exposure leads to very high CH_4 oxidation rates that attain very high levels in different soils. Prior exposure, therefore, needs to be considered when assessing a soil's CH_4 oxidation capacity, for example, for use in methane oxidation systems.
- Compaction strongly reduces air-filled porosity and hence diffusivity, reflecting in lowered soil depths to which O_2 can penetrate. In compacted soils, the active methanotrophic zone is pushed to the upper crust, which is more susceptible to adverse effects from saturation or desiccation and seasonally varying extreme temperatures. Also, the diminished soil volume must exhibit higher methane oxidation rates to oxidize the same CH_4 load as less compacted soil.
- Fir-wood biochar addition increases air-filled porosity and hence diffusivity and the depth to which O_2 can penetrate, partially mitigating the adverse effects of compaction.
- Sieved fir-wood biochar changes the soil's pore size distribution. Soil texture plays a vital role in how pore size distribution, gas and water transport, and water retention are affected by biochar amendment. Additional study is needed to determine if geometric shapes of biochar can change the interpores and pore size fractions between the solid particles altering soil tortuosity and/or contributing to water clogging, inhibiting oxygen penetration into the soil, and adversely impacting CH_4 oxidation.
- Fir-wood biochar addition can significantly change the methanotrophic community composition, with the response being soil-specific. MOB abundance and composition are unrelated to soil compaction and the corresponding changes in soil porosity. Also, they are indirectly linked to CH_4 oxidation rates, at least not at the level observed in this study.

Understanding the changes in biocover soil properties caused by the added materials is critical for designing efficient landfill covers and optimizing methane oxidation. Suppose fir-wood biochar produced at 500 °C is considered as an amendment to landfill cover soils to enhance methane oxidation of fugitive methane emissions. In that case, biochar is most effective in coarse soils rather than in fine soils with high clay contents.

CRediT authorship contribution statement

Susan Yi: Principal investigator, Conceptualization, Methodology, Investigation, Data analysis, Visualization, Writing of original draft. **Anne Heijbroek:** Investigation (Soil compaction). **Luis Cutz:** Investigation (Biochar surface properties), Review & editing of manuscript. **Stephanie Pillay:** Investigation (Microbial community analysis), Review & editing of manuscript. **Wiebren de Jong:** Review & editing of manuscript. **Thomas Abeel:** Methodology, Review & editing of manuscript. **Julia Gebert:** Conceptualization, Methodology, Data analysis & validation, Review & editing of manuscript, Funding acquisition, Supervision, Project administration, Resources.

Declaration of competing interest

Corresponding author and the co-authors declare that they have no known competing financial interests or personal relationships that could have appeared to influence the work reported in this paper.

Data availability

Data will be made available on request.

Acknowledgements

We greatly appreciate the funding from the Delft University of Technology Bioengineering Institute and the support from the National Research Foundation of South Africa (Grant Numbers: 120192). We thank the staff at TUDelft (Jens van den Berg, Michiel Slob, Karel Heller, Roland Klasen, and Ellen Meijvogel-de Koning) for technical assistance, securing supplies, and instrumental support. Without them, this study would not have been possible.

Appendix A. Supplementary data

Supplementary data to this article can be found online at https://doi.org/10.1016/j.scitotenv.2023.167951.

References

Amaral, J.A., Ren, T., Knowles, R., 1998. Atmospheric methane consumption by forest soils and extracted bacteria at different pH values. Appl. Environ. Microbiol. 64, 2397–2402. https://doi.org/10.1128/aem.64.7.2397-2402.1998.

Amoakwah, E., Frimpong, K.A., Okae-Anti, D., Arthur, E., 2017. Soil water retention, air flow and pore structure characteristics after corn cob biochar application to a tropical sandy loam. Geoderma 307, 189–197. https://doi.org/10.1016/j.geoderma.2017.08.025.

Andrews, S., 2013. FastQC: A quality control tool for High Throughput Sequence Data. Babraham Bioinformatics. https://www.bioinformatics.babraham.ac.uk/projects/fastqc/.

Anlauf, R., Rehrmann, P., 2012. Effect of compaction on soil hydraulic parameters of vegetative landfill covers. Geomaterials 2, 29–36. https://doi.org/10.4236/gm.2012.22005.

ASTM, 2006. Standard test method for sieve analysis of fine and coarse aggregates: C136-06. ASTM Int. https://doi.org/10.1520/C0136-06.

ASTM, 2021. Standard test methods for laboratory compaction characteristics of soil using standard effort: D698-1221. ASTM Int. https://doi.org/10.1520/D0698-12R21.

Bao, Z., Okubo, T., Kubota, K., Kasahara, Y., Tsurumaru, H., Anda, M., Ikeda, S., Minamisawa, K., 2014. Metaproteomic identification of diazotrophic methanotrophs and their localization in root tissues of field-grown rice plants. Appl. Environ. Microbiol. 80, 5043–5052. https://doi.org/10.1128/AEM.00969-14.

Berisso, F.E., Schjønning, P., Keller, T., Lamandé, M., Etana, A., de Jonge, L.W., Iversen, B.V., Arvidsson, J., Forkman, J., 2012. Persistent effects of subsoil

compaction on pore size distribution and gas transport in a loamy soil. Soil Tillage Res. 122, 42–51. https://doi.org/10.1016/j.still.2012.02.005.
Blake, G.R., 2008. Particle density. Encycl. Soil Sci. 504–505 https://doi.org/10.1007/978-1-4020-3995-9_406.
Bodelier, P.L.E., 2011. Interactions between nitrogenous fertilizers and methane cycling in wetland and upland soils. Curr. Opin. Environ. Sustain. 3, 379–388. https://doi.org/10.1016/j.cosust.2011.06.002.
Boeckx, P., Cleemput, O., Villaralvo, I., 1996. Methane emission from a landfill and the methane oxidising capacity of its covering soil. Soil Biol. Biochem. 28, 1397–1405. https://doi.org/10.1016/S0038-0717(96)00147-2.
Bolger, A.M., Lohse, M., Usadel, B., 2014. Trimmomatic: a flexible trimmer for Illumina sequence data. Bioinformatics 30, 2114–2120. https://doi.org/10.1093/bioinformatics/btu170.
Börjesson, G., Sundh, I., Svensson, B., 2004. Microbial oxidation of CH_4 at different temperatures in landfill cover soils. FEMS Microbiol. Ecol. 48, 305–312. https://doi.org/10.1016/j.femsec.2004.02.006.
Brtnicky, M., Datta, R., Holatko, J., Bielska, L., Gusiatin, Z.M., Kucerik, J., Hammerschmiedt, T., Danish, S., Radziemska, M., Mravcova, L., Fahad, S., Kintl, A., Sudoma, M., Ahmed, N., Pecina, V., 2021. A critical review of the possible adverse effects of biochar in the soil environment. Sci. Total Environ. 796, 148756 https://doi.org/10.1016/j.scitotenv.2021.148756.
Czepiel, P.M., Crill, P.M., Harriss, R.C., 1995. Environmental factors influencing the variability of methane oxidation in temperate zone soils. J. Geophys. Res. 100, 9359–9364. https://doi.org/10.1029/95JD00542.
Dane, J.H., Topp, G.C., 2002. Methods of Soil Analysis: Part 4, Physical methods, SSSA Book Series. Soil Science Society of America, Madison, WI. https://doi.org/10.2136/sssabookser5.4.
Das, O., Sarmah, A.K., Bhattacharyya, D., 2015. A novel approach in organic waste utilization through biochar addition in wood/polypropylene composites. Waste Manag. 38, 132–140. https://doi.org/10.1016/j.wasman.2015.01.015.
De Visscher, A., Thomas, D., Boeckx, P., Van Cleemput, O., 1999. Methane oxidation in simulated landfill cover soil environments. Environ. Sci. Technol. 33, 1854–1859. https://doi.org/10.1021/es9900961.
Del Grosso, M., Cutz, L., Tiringer, U., Tsekos, C., Taheri, P., de Jong, W., 2022. Influence of indirectly heated steam-blown gasification process conditions on biochar physico-chemical properties. Fuel Process. Technol. 235, 107347 https://doi.org/10.1016/j.fuproc.2022.107347.
Gebert, J., Groengroeft, A., Miehlich, G., 2003. Kinetics of microbial landfill methane oxidation in biofilters. Waste Manag. 23, 609–619. https://doi.org/10.1016/S0956-053X(03)00105-3.
Gebert, J., Singh, B.K., Pan, Y., Bodrossy, L., 2009. Activity and structure of methanotrophic communities in landfill cover soils. Environ. Microbiol. Rep. 1, 414–423. https://doi.org/10.1111/j.1758-2229.2009.00061.x.
Gebert, J., Groengroeft, A., Pfeiffer, E.M., 2011. Relevance of soil physical properties for the microbial oxidation of methane in landfill covers. Soil Biol. Biochem. 43, 1759–1767. https://doi.org/10.1016/j.soilbio.2010.07.004.
Gebert, J., Rachor, I., Streese, J., Pfeiffer, E.M., 2016. Methane oxidation in a landfill cover soil under conditions of diffusive and advective flux, assessed by in-situ and ex-situ methods. Curr. Environ. Eng. 3, 144–160. https://doi.org/10.2174/2212717803666160628093746.
Gebert, J., van Verseveld, C.J., Blom, H.P., Heimovaara, T.J., 2019. Effect of compaction and moisture on gas diffusivity and conductivity of soils for use in methane oxidation systems. In: Proceedings Sardinia 2019, 17th International Waste Management and Landfill Symposium, Sardinia, Italy.
Gebert, J., Huber-Humer, M., Cabral, A.R., 2022. Design of microbial methane oxidation systems for landfills. Front. Environ. Sci. https://doi.org/10.3389/fenvs.2022.907562.
Gebhardt, S., Fleige, H., Horn, R., 2009. Effect of compaction on pore functions of soils in a Saalean moraine landscape in North Germany. J. Plant Nutr. Soil Sci. 172, 688–695. https://doi.org/10.1002/jpln.200800073.
van Genuchten, M.T., 1980. A closed-form equation for predicting the hydraulic conductivity of unsaturated soils. Soil Sci. Soc. Am. J. 44, 892–898. https://doi.org/10.2136/sssaj1980.03615995004400050002x.
Gupta, S.C., Sharma, P.P., DeFranchi, S.A., 1989. Compaction effects on soil structure. Adv. Agron. 42, 311–338. https://doi.org/10.1016/S0065-2113(08)60528-3.
Hagen, G.H.L., 1839. Über die bewgung des wassers in engen cylindrischen röhren. Poggendorfs Ann. der Phys. und Chemie. 2, 423–442.
Hajnos, M., Lipiec, J., Swieboda, R., Sokolowska, Z., Witkowska-Walczak, B., 2006. Complete characterization of pore size distribution of tilled and orchard soil using water retention curve, mercury porosimetry, nitrogen adsorption, and water desorption methods. Geoderma 135, 307–314. https://doi.org/10.1016/j.geoderma.2006.01.010.
Hanson, R.S., Hanson, T.E., 1996. Methanotrophic bacteria. Microbiol. Rev. 60, 439–471. https://doi.org/10.1128/mmbr.60.2.439-471.1996.
Hilger, H.A., Wollum, A.G., Barlaz, M.A., 2000. Landfill methane oxidation response to vegetation, fertilization, and liming. J. Environ. Qual. 29, 324–334. https://doi.org/10.2134/jeq2000.00472425002900010041x.
Hill, R.A., Hunt, J., Sanders, E., Tran, M., Burk, G.A., Mlsna, T.E., Fitzkee, N.C., 2019. Effect of biochar on microbial growth: a metabolomics and bacteriological investigation in *E. coli*. Environ. Sci. Technol. 53, 2635–2646. https://doi.org/10.1021/acs.est.8b05024.
Holland, G., Gebert, J., 2020. Effect of compaction on gas transport through an agricultural soil used for a methane oxidation system. B.S. Thesis, Delft University of Technology Bachelor End Proj. Appl. Earth Sci. 15–32.
Horn, R., Smucker, A., 2005. Structure formation and its consequences for gas and water transport in unsaturated arable and forest soils. Soil Tillage Res. 82, 5–14. https://doi.org/10.1016/J.STILL.2005.01.002.
Huang, D., Yang, L., Ko, J.H., Xu, Q., 2019. Comparison of the methane-oxidizing capacity of landfill cover soil amended with biochar produced using different pyrolysis temperatures. Sci. Total Environ. 693 https://doi.org/10.1016/j.scitotenv.2019.133594.
Huber-Humer, M., Gebert, J., Hilger, H., 2008. Biotic systems to mitigate landfill methane emissions. Waste Manag. Res. 26, 33–46. https://doi.org/10.1177/0734242X07087977.
Hunt, D.E., Lin, Y., Church, M.J., Karl, D.M., Tringe, S.G., Izzo, L.K., Johnson, Z.I., 2013. Relationship between abundance and specific activity of bacterioplankton in open ocean surface waters. Appl. Environ. Microbiol. 79, 177–184. https://doi.org/10.1128/AEM.02155-12.
IPCC, 2021. Climate Change 2021: The Physical Science Basis. Contribution of Working Group I to the Sixth Assessment Report of the Intergovernmental Panel on Climate Change. Cambridge, United Kingdom and New York, NY, USA. https://doi.org/10.1017/9781009157896.
Jung, G.-Y., Rhee, S.-K., Han, Y.-S., Kim, S.-J., 2020. Genomic and physiological properties of a facultative methane-oxidizing bacterial strain of *Methylocystis* sp. from a wetland. Microorganisms 8. https://doi.org/10.3390/microorganisms8111719.
Keiblinger, K.M., Liu, D., Mentler, A., Zehetner, F., Zechmeister-Boltenstern, S., 2015. Biochar application reduces protein sorption in soil. Org. Geochem. 87, 21–24. https://doi.org/10.1016/j.orggeochem.2015.06.005.
Kightley, D., Nedwell, D.B., Cooper, M., 1995. Capacity for methane oxidation in landfill cover soils measured in laboratory-scale soil microcosms. Appl. Environ. Microbiol. 61, 592–601. https://doi.org/10.1128/aem.61.2.592-601.1995.
Lamprinakos, R., Manahiloh, K.N., 2019. Evaluating the compaction behavior of soils with biochar amendment. In: ASCE Geo-Congress 2019, GSP 390. https://doi.org/10.1061/9780784482117.013.
Lehmann, J., Joseph, S., 2009. Biochar for Environmental Management: Science and Technology. Earthscan, London; Sterling, VA.
Lipiec, J., Hajnos, M., Świeboda, R., 2012. Estimating effects of compaction on pore size distribution of soil aggregates by mercury porosimeter. Geoderma 179–180, 20–27. https://doi.org/10.1016/j.geoderma.2012.02.014.
Lu, J., Breitwieser, F.P., Thielen, P., Salzberg, S.L., 2017. Bracken: estimating species abundance in metagenomics data. PeerJ Comput. Sci. 3, e104 https://doi.org/10.7717/peerj-cs.104.
Marsiello, C.A., Dugan, B., Brewer, C.E., Spokas, K.A., Novak, J.M., Liu, Z., Sorrenti, G., 2015. Biochar effects on soil hydrology. In: Lehmann, J., Joseph, S. (Eds.), Biochar for Environmental Management: Science, Technology and Implementation, 2nd edition. Taylor and Francis, Florence, KY, USA, pp. 543–562.
Mckay, G., Pradhan, S., Mackey, H., Al-Ansari, T., 2021. Biochar: a sustainable approach for water stress and plant growth. Int. J. Glob. Warm. 25, 425. https://doi.org/10.1504/IJGW.2021.10042683.
Memetova, A., Tyagi, I., Karri, R.R., Kumar, V., Tyagi, K., Suhas, Memetov, N., Zelenin, A., Pasko, T., Gerasimova, A., Tarov, D., Dehghani, M.H., Singh, K., 2022. Porous carbon-based material as a sustainable alternative for the storage of natural gas (methane) and biogas (biomethane): a review. Chem. Eng. J. 446, 137373 https://doi.org/10.1016/j.cej.2022.137373.
Moldrup, P., Olesen, T., Komatsu, T., Schjonning, P., Rolston, D.E., 2001. Tortuosity, diffusivity, and permeability in the soil liquid and gaseous phases. Soil Sci. Soc. Am. J. 65, 613–623.
Moldrup, P., Olesen, T., Yoshikawa, S., Komatsu, T., McDonald, A.M., Rolston, D.E., 2005a. Predictive-descriptive models for gas and solute diffusion coefficients in variably saturated porous media coupled to pore-size distribution: III. Inactive pore space interpretations of gas diffusivity. Soil Sci. 170, 867–880. https://doi.org/10.1097/01.ss.0000196770.45951.06.
Moldrup, P., Olesen, T., Yoshikawa, S., Komatsu, T., Rolston, D.E., 2005b. Predictive-descriptive models for gas and solute diffusion coefficients in variably saturated porous media coupled to pore-size distribution: I. Gas diffusivity in repacked soil. Soil Sci. 170, 843–853. https://doi.org/10.1097/01.ss.0000196769.51788.73.
Mostafid, M.E., Shank, C., Imhoff, P.T., Yazdani, R., 2012. Gas transport properties of compost-woodchip and green waste for landfill biocovers and biofilters. Chem. Eng. J. 191, 314–325. https://doi.org/10.1016/j.cej.2012.03.022.
Nagler, M., Praeg, N., Niedrist, G.H., Attermeyer, K., Catalán, N., Pilotto, F., Gutmann Roberts, C., Bors, C., Fenoglio, S., Colls, M., Cauvy-Fraunié, S., Doyle, B., Romero, F., Machalett, B., Fuss, T., Bednařík, A., Klaus, M., Gilbert, P., Lamonica, D., Nydahl, A. C., Romero González-Quijano, C., Thuile Bistarelli, L., Kenderov, L., Piano, E., Mor, J., Evtimova, V., Deeyto, E., Freixa, A., Rulík, M., Pegg, J., Herrero Ortega, S., Steinle, L., Bodmer, P., 2021. Abundance and biogeography of methanogenic and methanotrophic microorganisms across European streams. J. Biogeogr. 48, 947–960. https://doi.org/10.1111/jbi.14052.
Nimmo, J.R., 2004. Porosity and pore size distribution. In: Encyclopedia of Soils in the Environment. Elsevier, London, pp. 295–303.
Park, J.R., Moon, S., Ahn, Y.M., Kim, J.Y., Nam, K., 2005. Determination of environmental factors influencing methane oxidation in a sandy landfill cover soil. Environ. Technol. 26, 93–102. https://doi.org/10.1080/09593332608618586.
Poiseuille, J.L.M., 1840. Physiques - recherches experimetales sur le mouvement des liquides dans les tubes de tres petits diametres. Acad. Des. Sci. Comptes Rendus 11 (961–967), 1041–1048.
Poulsen, T.G., Blendstrup, H., Schjonning, P., 2008. Air permeability in repacked porous media with variable structure-forming potential. Vadose Zone J. 7, 1139–1143. https://doi.org/10.2136/vzj2007.0147.

Pulat, H.F., Yukselen-Aksoy, Y., 2013. Compaction behavior of synthetic and natural MSW samples in different compositions. Waste Manag. Res. 31, 1255–1261. https://doi.org/10.1177/0734242X13507967.

Rachor, I.M., Gebert, J., Gröngröft, A., Pfeiffer, E.M., 2013. Variability of methane emissions from an old landfill over different time-scales. Eur. J. Soil Sci. 64, 16–26. https://doi.org/10.1111/ejss.12004.

Reddy, K., Yargicoglu, E., Yue, D., Yaghoubi, P., 2014. Enhanced microbial methane oxidation in landfill cover soil amended with biochar. J. Geotech. Geoenviron. Eng. 140, 1–11. https://doi.org/10.1061/(ASCE)GT.1943-5606.0001148.

Reddy, K., Yargicoglu, E., Chetri, J., 2021. Field-scale performance of biochar-amended soil covers for landfill methane oxidation. Biomass Convers. Biorefinery. https://doi.org/10.1007/s13399-021-01487-w.

RIVM, 2021. Greenhouse Gas Emissions in the Netherlands 1990–2019: National Inventory Report 2021. https://doi.org/10.21945/RIVM-2021-0007.

Rockhold, M.L., Yarwood, R.R., Selker, J.S., 2004. Coupled microbial and transport processes in soils. Vadose Zo. J. 3, 368–383. https://doi.org/10.2136/vzj2004.0368.

Romero, E., Jommi, C., 2008. An insight into the role of hydraulic history on the volume changes of anisotropic clayey soils. Water Resour. Res. 44 https://doi.org/10.1029/2007WR006558.

Röwer, I.U., Geck, C., Gebert, J., Pfeiffer, E.M., 2011. Spatial variability of soil gas concentration and methane oxidation capacity in landfill covers. Waste Manag. 31, 926–934. https://doi.org/10.1016/j.wasman.2010.09.013.

Sadasivam, B.Y., Reddy, K.R., 2015. Adsorption and transport of methane in biochars derived from waste wood. Waste Manag. 43, 218–229. https://doi.org/10.1016/j.wasman.2015.04.025.

Scheutz, C., Kjeldsen, P., 2004. Environmental factors influencing attenuation of methane and hydrochlorofluorocarbons in landfill cover soils. J. Environ. Qual. 33, 72–79. https://doi.org/10.2134/jeq2004.7200.

Scheutz, C., Kjeldsen, P., Bogner, J.E., De Visscher, A., Gebert, J., Hilger, H.A., Huber-Humer, M., Spokas, K., 2009. Microbial methane oxidation processes and technologies for mitigation of landfill gas emissions. Waste Manag. Res. 27, 409–455. https://doi.org/10.1177/0734242X09339325.

Schjonning, P., Thomsen, I.K., Moldrup, P., Christensen, B.T., 2003. Linking soil microbial activity to water- and air-phase contents and diffusivities. Soil Sci. Soc. Am. J. 67, 156–165.

Sleutel, S., Bouckaert, L., Buchan, D., Van Loo, D., Cornelis, W.M., Sanga, H.G., 2012. Manipulation of the soil pore and microbial community structure in soil mesocosm incubation studies. Soil Biol. Biochem. 45, 40–48. https://doi.org/10.1016/j.soilbio.2011.09.016.

Spokas, K.A., Bogner, J.E., 2011. Limits and dynamics of methane oxidation in landfill cover soils. Waste Manag. 31, 823–832. https://doi.org/10.1016/J.WASMAN.2009.12.018.

Stokes, G.G., 1845. On the theories of the internal friction of fluids in motion, and of the equilibrium and motion of elastic solids. Trans. Cambridge Philos. Soc. 8, 287–341.

Sun, Z., Moldrup, P., Elsgaard, L., Arthur, E., Bruun, E.W., Hauggaard-Nielsen, H., de Jonge, L.W., 2013. Direct and indirect short-term effects of biochar on physical characteristics of an arable sandy loam. Soil Sci. 178, 465–473. https://doi.org/10.1097/SS.0000000000000010.

US EPA. Revisions to Criteria for Municipal Solid Waste Landfills, Federal Register, 40 CFR Part 258. https://www.govinfo.gov/content/pkg/FR-1997-07-29/pdf/97-19942.pdf.

Vereecken, H., Maes, J., Feyen, J., Darius, P., 1989. Estimating the soil moisture retention characteristic from texture, bulk density, and carbon content. Soil Sci. 148 https://doi.org/10.1097/00010694-198912000-00001.

Verseveld, C., 2018. Gas Flow Through Methane Oxidation Systems: A Laboratory and Numerical Study for Optimising System Design. Delft University of Technology.

Verseveld, C.J.W., Gebert, J., 2020. Effect of compaction and soil moisture on the effective permeability of sands for use in methane oxidation systems. Waste Manag. 107, 44–53. https://doi.org/10.1016/j.wasman.2020.03.038.

Watabe, Y., Leroueil, S., Le Bihan, J.-P., 2000. Influence of compaction conditions on pore-size distribution and saturated hydraulic conductivity of a glacial till. Can. Geotech. J. 37, 1184–1194. https://doi.org/10.1139/t00-053.

Wickramarachchi, P., Kawamoto, K., Hamamoto, S., Nagamori, M., Moldrup, P., Komatsu, T., 2011. Effects of dry bulk density and particle size fraction on gas transport parameters in variably saturated landfill cover soil. Waste Manag. 31, 2464–2472. https://doi.org/10.1016/j.wasman.2011.07.008.

Wilshusen, J.H., Hettiaratchi, J.P.A., De Visscher, A., Saint-Fort, R., 2004. Methane oxidation and formation of EPS in compost: effect of oxygen concentration. Environ. Pollut. 129, 305–314. https://doi.org/10.1016/j.envpol.2003.10.015.

Wood, D.E., Lu, J., Langmead, B., 2019. Improved metagenomic analysis with Kraken 2. Genome Biol. 20, 257. https://doi.org/10.1186/s13059-019-1891-0.

Yargicoglu, E., Reddy, K., 2017a. Microbial abundance and activity in biochar-amended landfill cover soils: evidence from large-scale column and field experiments. J. Environ. Eng. 143 https://doi.org/10.1061/(ASCE)EE.1943-7870.0001254.

Yargicoglu, E., Reddy, K., 2017b. Effects of biochar and wood pellets amendments added to landfill cover soil on microbial methane oxidation: a laboratory column study. J. Environ. Manag. 193, 19–31. https://doi.org/10.1016/j.jenvman.2017.01.068.

Yargicoglu, E., Reddy, K., 2018. Biochar-amended soil cover for microbial methane oxidation: effect of biochar amendment ratio and cover profile. J. Geotech. Geoenviron. Eng. 144, 1–15. https://doi.org/10.1061/(ASCE)GT.1943-5606.0001845.

Yi, S., Witt, B., Chiu, P., Guo, M., Imhoff, P., 2015. The origin and reversible nature of poultry litter biochar hydrophobicity. J. Environ. Qual. 44 https://doi.org/10.2134/jeq2014.09.0385.

Yi, S., Chang, N.Y., Imhoff, P.T., 2020. Predicting water retention of biochar-amended soil from independent measurements of biochar and soil properties. Adv. Water Resour. 142, 103638 https://doi.org/10.1016/J.ADVWATRES.2020.103638.